JSTT JOURNAL OF SCIENCE AND TRANSPORT TECHNOLOGY

Journal of Science and Transport Technology
Journal homepage: https://jstt.vn/index.php/en

UNIVERSITY OF TRANSPORT TECHNOLOGY

An analytical approach for nonlinear thermo-mechanical buckling behavior of Porous FG-GPLRC circular plates and spherical caps

Nguyen Thi Phuong[1,2], Vu Hoai Nam[3], Bui Tien Tu[4,5,*]

[1]Mechanics of Advanced Materials and Structures, Institute for Advanced Study in Technology, Ton Duc Thang University, Ho Chi Minh City, Vietnam; nguyenthiphuong@tdtu.edu.vn

[2]Faculty of Civil Engineering, Ton Duc Thang University, Ho Chi Minh City, Vietnam

[3]Faculty of Civil Engineering, University of Transport Technology, Hanoi, Vietnam

[4]Institute of Transport Technology, University of Transport Technology, Hanoi, Vietnam

[5]Faculty of Fundamental Science for Engineering, University of Transport Technology, Hanoi, Vietnam

Article info
Type of article:
Original research paper

DOI:
https://doi.org/10.58845/jstt.utt.2025.en.5.1.40-60

***Corresponding author:**
Email address:
tubt@utt.edu.vn

Received: 02/01/2025
Received in Revised Form: 28/02/2025
Accepted: 10/03/2025

Abstract: This paper presents an analytical approach for the nonlinear thermo-mechanical stability analysis of porous functionally graded graphene platelets reinforced composite (Pr-FG-GPLRC) circular plates (CPs) and shallow spherical caps (SCs) resting on nonlinear elastic foundation. Pr-FG-GPLRC is considered to have three different types of foam distribution. The applied load includes uniform external pressure and uniform thermal loads. The governing formulations are established by the first-order shear deformation theory (FSDT) and the von Kármán geometrical nonlinearities. The deformation compatibility equations are established and the stress function is introduced to reduce the equilibrium equation system into three equations with three function variables (deflection, rotation, and stress function). The chosen solution form approximately satisfies the clamped boundary conditions and the Ritz energy method is applied to obtain the equilibrium equation system in nonlinear algebraic form. The explicit expressions of buckling loads and thermo-mechanical post-buckling curves can be obtained. Numerical investigations are performed to discuss the remarkable effects of nonlinear foundation stiffness, material, and geometrical properties imperfection on the nonlinear thermo-mechanical buckling behavior and load-carrying capacity of CPs and SCs.

Keywords: First-order shear deformation theory; Pr-FG-GPLRC; Shallow spherical caps; Ritz energy method; Nonlinear buckling and post-buckling; Nonlinear elastic foundation.

1. Introduction

The outstanding advantages in terms of load-bearing capacity, aesthetics, and expanding usable space of shallow spherical cap structures make them increasingly popular in engineering designs such as industrial and construction works. The combination of this structure with composite materials has attracted the attention of many domestic and foreign researchers on thermo-mechanical behavior.

Functionally graded materials (FGM) are typical advanced composite materials that combine the beneficial properties of two-component materials, ceramic and metal while overcoming the delamination disadvantages of classical composite materials. FGM has a wide range of applications in engineering design. FGM plate and shell structures have achieved many important research results on static and dynamic stability. The analysis of thermo-mechanical behavior of FGM spherical caps based on classical shell theory and first-order shear deformation theory was carried out by Shahsiah et al. [1] with the problem of nonlinear static instability; Boroujerdy and Eslami [2, 3] with the influence of piezoelectric layers on the nonlinear axisymmetric behavior; Moosaie and Panahi-Kalus [4] with thermal stress and Phuong et al. [5] with nonlinear vibration. In Vietnam, the FGM spherical caps with material properties dependent on temperature, axisymmetric deformation, considering geometric nonlinearity and initial imperfections, placed on elastic foundations were studied by Duc et al. [6], Bich et al. [7], Tung et al. [8, 9] with explicit expressions of critical loads and load-deflection relationships using the Galerkin method.

Functionally graded graphene platelets reinforced composite (FG-GPLRC) is the next potential material with outstanding mechanical properties that are being studied for application in important plate and shell structures. Many types of FG-GPLRC plate and shell structures have been studied so far in bending, buckling, and vibration problems, such as rectangular plates [10, 11], irregular quadrilateral plates [12], cylindrical panels [13], double-curvature shells [14] and annular plates [15, 16]. The number of publications on FG-GPLRC CP and SC structures is still insufficient due to their mathematical complexity. Ly et al. [17] used the high-order shear deformation theory and the Ritz method to analyze the nonlinear thermo-mechanical stability of sandwich FG-GPLRC CPs and SCs. Also using the Ritz method to solve the problem, Phuong et al. [18] analyzed the static stability of FG-GPLRC CPs and SCs placed on a nonlinear elastic foundation. In addition, Nam et al. [19] used the Rizt method to analyze the nonlinear thermo-mechanical stability of the FG-GPLRC CPs and SCs stiffened by spiderweb stiffeners. Liu et al. [20] analyzed the free vibration and bending of FG-GPLRC spherical shells using three-dimensional elasticity solutions.

Pr-FG-GPLRC with foam sizes distributed according to certain rules in the direction of structural thickness has many advantages in terms of sound insulation and heat insulation [21-24]. However, studies on the thermo-mechanical behavior of Pr-FG-GPLRC CPs and SCs are still limited.

This is the motivation for the researcher to conduct the first studies on the nonlinear stability of Pr-FG-GPLRC CP and SC structures using the stress function approach combined with the Ritz method in this study to contribute to the improvement of the thermo-mechanical behavior of this potential structure.

2. Model of Pr-FG-GPLRC circular plates and shallow spherical caps on nonlinear elastic foundation

Fig. 1 shows the FG-GPLRC CPs and SCs placed on a nonlinear elastic foundation with three coefficients K_1, K_2, K_3. The geometrical parameters of the caps include thickness h, main radius R, and base radius a. The caps are subjected to uniformly distributed external pressure q and uniformly distributed thermal load ΔT either in combination or separately. The deformation of the caps is assumed to be axisymmetric.

The Pr-FG-GPLRC is designed with a uniform distribution of GPLs and three different distributions of foam (PF-U, PF-X, and PF-O). The Young modulus $E(z)$ and mass density $\rho(z)$ of the structure are determined corresponding to the three types of foam as follows

$$E(z)=\begin{cases} e_U E_s, & \text{PF-U} \\ E_s - e_O E_s \cos\left(\dfrac{\pi z}{h}\right), & \text{PF-O} \\ E_s - e_X E_s\left[1-\cos\left(\dfrac{\pi z}{h}\right)\right], & \text{PF-X} \end{cases} \quad (1)$$

$$\rho(z)=\begin{cases} \rho_s \lambda_U, & \text{PF-U} \\ \rho_s - \lambda_O \rho_s \cos\left(\dfrac{\pi z}{h}\right), & \text{PF-O} \\ \rho_s - \lambda_X \rho_s\left[1-\cos\left(\dfrac{\pi z}{h}\right)\right], & \text{PF-X} \end{cases} \quad (2)$$

where E_s and ρ_s are respectively the Young modulus and mass density of the Pr-FG-GPLRC with zero porosity; e_U, e_O and e_X are foam coefficients, ρ_U, ρ_O and ρ_X are mass density coefficients.

The extended Halpin-Tsai model is used to determine E_s, as

$$E_s = \frac{3(1+\zeta_1\delta_1 V_{Gr})}{8(1-\delta_1 V_{Gr})}E_m + \frac{5(1+\zeta_2\delta_2 V_{Gr})}{8(1-\delta_2 V_{Gr})}E_{m,} \quad (3)$$

where

$$\delta_1 = \frac{(E_{Gr}/E_m)-1}{(E_{Gr}/E_m)+\zeta_1}, \delta_2 = \frac{(E_{Gr}/E_m)-1}{(E_{Gr}/E_m)+\zeta_2},$$
$$\zeta_1 = 2\left(\frac{a_{Gr}}{t_{Gr}}\right), \zeta_2 = 2\left(\frac{b_{Gr}}{t_{Gr}}\right), \quad (4)$$

$$V_{Gr} = \frac{W_{Gr}}{W_{Gr} + (\rho_{Gr}/\rho_m)(1-W_{Gr})}, \quad (5)$$

with V_{Gr} and W_{Gr} are the volume fraction and mass fraction, respectively of graphene platelets (GPLs); E_m and E_{Gr} are the elastic modulus of the matrix and GPLs, respectively; a_{Gr}, b_{Gr}, and t_{Gr} are the length, width, and thickness of GPLs, respectively; ρ_m and ρ_{Gr} are the densities of the matrix and GPLs, respectively.

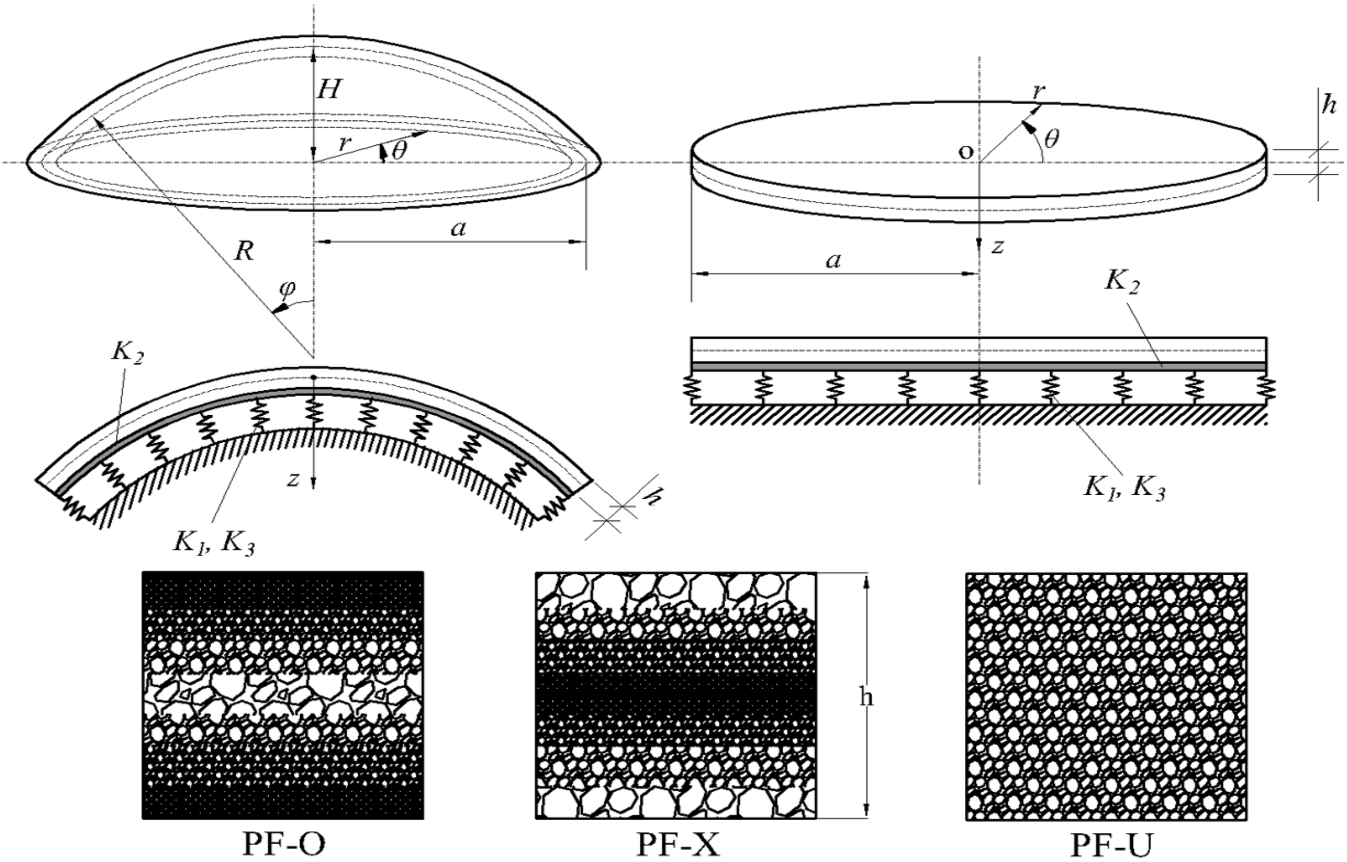

Fig. 1. Classification of Pr-FG-GPLRC and model of CPs and SCs

The typical mechanical property of Pr-FG-GPLRC are expressed by [22,23]

$$\frac{E(z)}{E_s} = \left[\frac{\rho(z)}{\rho_s}\right]^{2.73}, \tag{6}$$

By substituting Eq. (1) and Eq. (2) into Eq. (6), the relationship between the foam coefficients and mass density coefficients of Pr-FG-GPLRC can be obtained as

$$\begin{cases} \sqrt[2.73]{e_U} = \lambda_U, & \text{PF-U} \\ \sqrt[2.73]{1 - e_O \cos\left(\frac{\pi z}{h}\right)} = 1 - \lambda_O \cos\left(\frac{\pi z}{h}\right), & \text{PF-O} \\ \sqrt[2.73]{1 - e_X \left[1 - \cos\left(\frac{\pi z}{h}\right)\right]} & \\ = 1 - \lambda_X \left[1 - \cos\left(\frac{\pi z}{h}\right)\right], & \text{PF-X} \end{cases} \tag{7}$$

From Eq. (7), the mass of each type of pr-FG-GPLRC structure with different foam distributions is equal, leading to

$$\begin{aligned} &\int_0^{h/2} \sqrt[2.73]{1 - e_O \cos\left(\frac{\pi z}{h}\right)} dz \\ &= \int_0^{h/2} \sqrt[2.73]{e_U} dz = \int_0^{h/2} \sqrt[2.73]{1 - e_X \left[1 - \cos\left(\frac{\pi z}{h}\right)\right]} dz. \end{aligned} \tag{8}$$

The Poisson's ratio ν and thermal expansion α of the Pr-FG-GPLRC are constant and independent of the foams, determined by the rule of mixture, as

$$\begin{aligned} \nu &= \nu_m (1 - V_{Gr}) + \nu_{Gr} V_{Gr}, \\ \alpha &= \alpha_m (1 - V_{Gr}) + \alpha_{Gr} V_{Gr}. \end{aligned} \tag{9}$$

3. Formulation and solving method

The governing equations and resulting expressions are established based on FSDT applied to Pr-FG-GPLRC SC placed on a nonlinear elastic foundation subjected to mechanical and thermal loads, the results for the circular plate are obtained correspondingly when the main radius $R = \infty$.

The relationship between the displacement components at the point with coordinate z $(\bar{u}, \bar{v}, \bar{w})$ and at the corresponding point at the middle surface (u, v, w) of the shell in the φ, θ and z directions, respectively, is expressed as

$$\begin{aligned} \bar{u}(r,z) &= u(r) + \psi(r) z, \\ \bar{v}(r,z) &= 0, \\ \bar{w}(r,z) &= w(r) + w^*(r), \end{aligned} \tag{10}$$

where $\psi(r)$ is the rotation of the normal to the mid-surface and $w^*(r)$ is the geometrical imperfection of the shell.

The strain components of the shell at any point are

$$\begin{Bmatrix} \varepsilon_r \\ \varepsilon_\theta \\ \varepsilon_{rz} \end{Bmatrix} = \begin{Bmatrix} \varepsilon_r^0 + z\chi_r \\ \varepsilon_\theta^0 + z\chi_\theta \\ \psi + w_{,r} \end{Bmatrix}, \tag{11}$$

in which ε_r^0, ε_θ^0 and χ_r, χ_θ are strains at the mid-surface and curvatures, respectively, are determined as

$$\begin{Bmatrix} \varepsilon_r^0 \\ \varepsilon_\theta^0 \\ \chi_r \\ \chi_\theta \end{Bmatrix} = \begin{Bmatrix} -w\frac{1}{R} + \frac{w_{,r}^2}{2} + u_{,r} + w_{,r}^* w_{,r} \\ -w\frac{1}{R} + u\frac{1}{r} \\ \psi_{,r} \\ \psi\frac{1}{r} \end{Bmatrix}. \tag{12}$$

The Hooke law applies in this case as follows

$$\begin{aligned} \begin{Bmatrix} \sigma_r \\ \sigma_\theta \end{Bmatrix} &= \frac{E(z)}{1-\nu^2} \begin{Bmatrix} 1 & \nu \\ \nu & 1 \end{Bmatrix} \begin{Bmatrix} \varepsilon_r \\ \varepsilon_\theta \end{Bmatrix} \\ &\quad - \frac{E(z)}{1-\nu} \alpha(z) \begin{Bmatrix} \Delta T \\ \Delta T \end{Bmatrix}, \\ \sigma_{rz} &= \frac{E(z)}{2(1+\nu)} \varepsilon_{rz}. \end{aligned} \tag{13}$$

The expression of internal forces of the structures obtained

$$\begin{Bmatrix} N_r \\ N_\theta \\ M_r \\ M_\theta \end{Bmatrix} = \begin{Bmatrix} A_{11} & A_{12} & B_{11} & B_{12} \\ A_{21} & A_{22} & B_{21} & B_{22} \\ B_{11} & B_{12} & D_{11} & D_{12} \\ B_{21} & B_{22} & D_{21} & D_{22} \end{Bmatrix} \begin{Bmatrix} \varepsilon_r^0 \\ \varepsilon_\theta^0 \\ \chi_r \\ \chi_\theta \end{Bmatrix} - \begin{Bmatrix} \Phi_{1r} \\ \Phi_{1\theta} \\ \Phi_{2r} \\ \Phi_{2\theta} \end{Bmatrix} \Delta T, \quad Q_r = K_s H_{44} (\psi + w_{,r}), \tag{14}$$

in which

$$\left(H_{ij},A_{ij},B_{ij},D_{ij}\right)=\int_{-\frac{h}{2}}^{\frac{h}{2}}Q_{ij}\left(1,1,z,z^2\right)dz,$$

$$\Phi_{1r}=\int_{-\frac{h}{2}}^{\frac{h}{2}}\left(Q_{11}\alpha+Q_{12}\alpha\right)dz,$$

$$\Phi_{2r}=\int_{-\frac{h}{2}}^{\frac{h}{2}}\left(Q_{11}\alpha+Q_{12}\alpha\right)zdz,$$

$$\Phi_{1\theta}=\int_{-\frac{h}{2}}^{\frac{h}{2}}\left(Q_{21}\alpha+Q_{22}\alpha\right)dz,$$

$$\Phi_{2\theta}=\int_{-\frac{h}{2}}^{\frac{h}{2}}\left(Q_{21}\alpha+Q_{22}\alpha\right)zdz,Q_{44}=\frac{E(z)}{2\left[\nu(z)+1\right]},$$

$$Q_{11}=Q_{22}=\frac{E(z)}{1-\left[\nu(z)\right]^2},$$

$$Q_{12}=Q_{21}=\nu(z)\frac{E(z)}{1-\left[\nu(z)\right]^2}.$$

The shear correction factor is chosen according to the common value $K_s=5/6$. The ε_r^0, ε_θ^0 expression is derived from Eq. (14), as

$$\begin{bmatrix}\varepsilon_r^0\\ \varepsilon_\theta^0\end{bmatrix}=\begin{bmatrix}A_{11}^*N_r+B_{11}^*\chi_r+B_{12}^*\chi_\theta+A_{12}^*N_\theta-\Delta T\Phi_{1r}^*\\ A_{21}^*N_r+B_{21}^*\chi_r+B_{22}^*\chi_\theta+A_{22}^*N_\theta-\Delta T\Phi_{1\theta}^*\end{bmatrix}, \quad (15)$$

where

$$A_{11}^*=\frac{A_{22}}{A_{11}A_{22}-A_{12}A_{21}},A_{12}^*=\frac{-A_{12}}{A_{11}A_{22}-A_{12}A_{21}},$$

$$B_{11}^*=\frac{\left(A_{12}B_{21}-A_{22}B_{11}\right)}{A_{11}A_{22}-A_{12}A_{21}},B_{12}^*=\frac{\left(A_{12}B_{22}-A_{22}B_{12}\right)}{A_{11}A_{22}-A_{12}A_{21}},$$

$$A_{21}^*=\frac{-A_{21}}{A_{11}A_{22}-A_{12}A_{21}},A_{22}^*=\frac{A_{11}}{A_{11}A_{22}-A_{12}A_{21}},$$

$$B_{21}^*=\frac{\left(A_{11}B_{21}-A_{21}B_{11}\right)}{A_{12}A_{21}-A_{11}A_{22}},B_{22}^*=\frac{\left(A_{11}B_{22}-A_{21}B_{12}\right)}{A_{12}A_{21}-A_{11}A_{22}},$$

$$\Phi_{1r}^*=\frac{A_{12}\Phi_{1\theta}-A_{22}\Phi_{1r}}{A_{11}A_{22}-A_{12}A_{21}},\Phi_{1\theta}^*=\frac{A_{21}\Phi_{1r}-A_{11}\Phi_{1\theta}}{A_{11}A_{22}-A_{12}A_{21}}.$$

By substituting Eq. (15) into Eq. (14), the expression M_r,M_θ can be obtained as

$$\begin{bmatrix}M_r\\ M_\theta\end{bmatrix}=\begin{bmatrix}C_{11}^*N_r+D_{11}^*\chi_r+D_{12}^*\chi_\theta+C_{12}^*N_\theta-\Delta T\Phi_{2r}^*\\ C_{21}^*N_r+D_{21}^*\chi_r+D_{22}^*\chi_\theta+C_{22}^*N_\theta-\Delta T\Phi_{2\theta}^*\end{bmatrix}, \quad (16)$$

where

$$C_{11}^*=B_{11}A_{11}^*+B_{12}A_{21}^*,C_{12}^*=B_{11}A_{12}^*+B_{12}A_{22}^*,$$
$$D_{11}^*=B_{11}B_{11}^*+B_{12}B_{21}^*+D_{11},$$
$$D_{12}^*=B_{11}B_{12}^*+B_{12}B_{22}^*+D_{12},$$
$$C_{21}^*=B_{21}A_{11}^*+B_{22}A_{21}^*,C_{22}^*=B_{21}A_{12}^*+B_{22}A_{22}^*,$$
$$D_{21}^*=B_{21}B_{11}^*+B_{22}B_{21}^*+D_{21},$$
$$D_{22}^*=B_{21}B_{12}^*+B_{22}B_{22}^*+D_{22},$$
$$\Phi_{2r}^*=B_{11}\Phi_{1r}^*+B_{12}\Phi_{1\theta}^*+\Phi_{2r},$$
$$\Phi_{2\theta}^*=B_{21}\Phi_{1r}^*+B_{22}\Phi_{1\theta}^*+\Phi_{2\theta},$$

The strain compatibility equation of an imperfect spherical cap is expressed as

$$\frac{1}{r}\varepsilon_{r,r}^0-\varepsilon_{\theta,rr}^0-\frac{2}{r}\varepsilon_{\theta,r}^0=\frac{1}{Rr}\left(rw_{,rr}+w_{,r}\right)+\left(w_{,r}^*w_{,rr}+w_{,rr}w_{,r}+w_{,rr}^*w_{,r}\right)\frac{1}{r}. \quad (17)$$

The stress function $f(r)$ is defined to satisfy the following conditions

$$N_r=\frac{f_{,r}}{r},\quad N_\theta=f_{,rr}. \quad (18)$$

Considering the symmetry across the mid-surface of the Pr-FG-GPLRC, substituting Eq. (18) into Eq. (15), and then the resulting equations are substituted into Eq. (17), the compatibility equation is obtained

$$-A_{22}^*f_{,rrrr}+\frac{f_{,rrr}\left(A_{12}^*-A_{21}^*-2A_{22}^*\right)}{r}+\frac{f_{,rr}A_{11}^*}{r^2}-\frac{f_{,r}A_{11}^*}{r^3}=\frac{1}{R}\left(\frac{w_{,r}}{r}+w_{,rr}\right)+\left(w_{,r}^*w_{,rr}+w_{,r}w_{,rr}+w_{,rr}^*w_{,r}\right)\frac{1}{r}. \quad (19)$$

Substituting Eq. (18) into Eq. (16) results in

$$M_r=\frac{f_{,r}C_{11}^*}{r}+D_{11}^*\chi_r-\Delta T\Phi_{2r}^*+D_{12}^*\chi_\theta+C_{12}^*f_{,rr}, \quad (20)$$

$$M_\theta = \frac{f_{,r}C_{21}^*}{r} + D_{21}^*\chi_r - \Delta T\Phi_{2\theta}^* + D_{22}^*\chi_\theta + C_{22}^* f_{,rr}.$$

The Pr-FG-GPLRC spherical cap is considered to be axisymmetric deformed and clamped at the boundary edge. The boundary conditions at the center ($r = 0$) and the edge ($r = a$) are expressed as

$$\begin{aligned} &r = 0: \ \psi = 0, \quad f_{,r} = N_r r = 0, \\ &r = a: \ w = 0, \ \psi = 0, \quad N_r = Q_0, \end{aligned} \tag{21}$$

where Q_0 is compressive stress due to the clamped and immovable edge.

Based on boundary conditions (21), approximate solutions for the displacement component and rotation are

$$\begin{aligned} &\psi = \Psi \frac{r(a^2 - r^2)}{a^3}, \\ &w = W\frac{(a^2 - r^2)^2}{a^4}, w^* = W^* \frac{(a^2 - r^2)^2}{a^4}. \end{aligned} \tag{22}$$

where W and Ψ are maximal displacement constituent and rotation, W^* is maximal imperfection.

Substituting Eq. (22) into Eq. (19), then some mathematical transformations are applied to obtain the stress function, as

$$f_{,r} = Y_1 r^7 + Y_2 r^5 + Y_3 r^3 + Y_4 r^2 + Y_5 r, \tag{23}$$

where

$$\begin{aligned} &Y_1 = Y_{11}W^2 + Y_{12}WW^*, \\ &Y_2 = Y_{21}W^2 + Y_{22}WW^* + Y_{23}W, \\ &Y_3 = Y_{31}W^2 + Y_{32}WW^* + Y_{33}W, \\ &Y_4 = 0, \\ &Y_5 = Y_{51}W^2 + Y_{53}WW^* + Y_{52}W + Q_0, \\ &Y_{11} = \frac{8}{a^8\left(-7A_{21}^* + 7A_{12}^* - 49A_{22}^* + A_{11}^*\right)}, \\ &Y_{12} = \frac{16}{a^8\left(-7A_{21}^* + 7A_{12}^* - 49A_{22}^* + A_{11}^*\right)}, \\ &Y_{21} = -\frac{16}{a^6\left(-5A_{21}^* + 5A_{12}^* - 25A_{22}^* + A_{11}^*\right)}, \\ &Y_{22} = -\frac{32}{a^6\left(-5A_{21}^* + 5A_{12}^* - 25A_{22}^* + A_{11}^*\right)}, \\ &Y_{23} = \frac{4}{R\left(-5A_{21}^* + 5A_{12}^* - 25A_{22}^* + A_{11}^*\right)a^4}, \\ &Y_{31} = \frac{8}{\left(-3A_{21}^* + 3A_{12}^* - 9A_{22}^* + A_{11}^*\right)a^4}, \\ &Y_{32} = \frac{16}{\left(-3A_{21}^* + 3A_{12}^* - 9A_{22}^* + A_{11}^*\right)a^4}, \\ &Y_{33} = -\frac{4}{R\left(-3A_{21}^* + 3A_{12}^* - 9A_{22}^* + A_{11}^*\right)a^2}, \\ &Y_{51} = -\frac{1}{a^2}\left[\frac{8}{\left(-7A_{21}^* + 7A_{12}^* - 49A_{22}^* + A_{11}^*\right)} - \frac{16}{\left(-5A_{21}^* + 5A_{12}^* - 25A_{22}^* + A_{11}^*\right)} + \frac{8}{\left(-3A_{21}^* + 3A_{12}^* - 9A_{22}^* + A_{11}^*\right)}\right], \\ &Y_{52} = \frac{4}{R\left(-3A_{21}^* + 3A_{12}^* - 9A_{22}^* + A_{11}^*\right)} - \frac{4}{R\left(-5A_{21}^* + 5A_{12}^* - 25A_{22}^* + A_{11}^*\right)}, \\ &Y_{53} = -\frac{1}{a^2}\left[\frac{16}{\left(-7A_{21}^* + 7A_{12}^* - 49A_{22}^* + A_{11}^*\right)} - \frac{32}{\left(-5A_{21}^* + 5A_{12}^* - 25A_{22}^* + A_{11}^*\right)} + \frac{16}{\left(-3A_{21}^* + 3A_{12}^* - 9A_{22}^* + A_{11}^*\right)}\right], \end{aligned}$$

and Q_0 is determined by the average end-shortening displacement condition $\Delta = 0$ at the edge, as

$$\Delta = -\frac{1}{2\pi a^2}\int_0^{2\pi}\int_0^a u_{,r} r dr d\theta = 0. \tag{24}$$

leading to

$$\begin{aligned} Q_0 = \frac{1}{12U_{44}}\Big[&-\left(4U_{23}a^4 + 6U_{33}a^2 + 12U_{43}\right)W \\ &-\left(3U_{11}a^6 + 4U_{21}a^4 + 6U_{31}a^2 + 12U_{41}\right)W^2 \\ &-\left(3a^6U_{12} + 4U_{22}a^4 + 6a^2U_{32} + 12U_{42}\right)WW^* \\ &-\left(6U_{34}a^2 + 12U_{46}\right)\Psi - 12U_{45}\Delta T\Big]. \end{aligned} \tag{25}$$

where

$$U_{11}=\frac{7a^8A_{12}Y_{11}+8A_{22}A_{11}-8A_{21}A_{12}-a^8Y_{11}A_{22}}{-a^8A_{22}A_{11}+a^8A_{21}A_{12}},$$

$$U_{12}=\frac{7a^8Y_{12}A_{12}+16A_{22}A_{11}-16A_{21}A_{12}-a^8A_{22}Y_{12}}{-a^8A_{22}A_{11}+a^8A_{21}A_{12}},$$

$$U_{21}=\frac{5a^6Y_{21}A_{12}-16A_{11}A_{22}+16A_{21}A_{12}-a^6A_{22}Y_{21}}{-a^6A_{22}A_{11}+a^6A_{21}A_{12}},$$

$$U_{22}=\frac{5a^6Y_{22}A_{12}-32A_{11}A_{22}+32A_{21}A_{12}-a^6A_{22}Y_{22}}{-a^6A_{11}A_{22}+a^6A_{12}A_{21}},$$

$$U_{23}=\frac{5A_{12}Y_{23}-A_{22}Y_{23}}{-A_{22}A_{11}+A_{21}A_{12}}-\frac{1}{a^4R},$$

$$U_{31}=\frac{\left(-A_{22}Y_{31}+3Y_{31}A_{12}\right)-(8A_{21}A_{12}-A_{22}A_{11})}{\left(A_{12}A_{21}-A_{22}A_{11}\right)},$$

$$U_{32}=\frac{\left(6Y_{32}A_{12}-2A_{22}Y_{32}\right)+32\left(A_{11}A_{22}-A_{21}A_{12}\right)}{\left(-2A_{11}A_{22}+2A_{12}A_{21}\right)},$$

$$U_{33}=\frac{3A_{12}Y_{33}-A_{22}Y_{33}}{A_{12}A_{21}-A_{11}A_{22}}+\frac{2A_{11}A_{22}-2A_{21}A_{12}}{a^2\left(A_{12}A_{21}-A_{11}A_{22}\right)R},$$

$$U_{34}=\frac{2A_{12}\left(3B_{21}+B_{22}\right)-6A_{22}B_{11}-2A_{22}B_{12}}{a^3\left(-2A_{11}A_{22}+2A_{12}A_{21}\right)},$$

$$U_{41}=\frac{A_{12}Y_{51}-A_{22}Y_{51}}{A_{21}A_{12}-A_{22}A_{11}},U_{42}=\frac{A_{12}Y_{53}-A_{22}Y_{53}}{A_{21}A_{12}-A_{22}A_{11}},$$

$$U_{43}=\frac{A_{12}Y_{52}-A_{22}Y_{52}}{A_{21}A_{12}-A_{22}A_{11}}+\frac{1}{R},$$

$$U_{44}=\frac{-A_{22}+A_{12}}{A_{21}A_{12}-A_{22}A_{11}},U_{45}=\frac{A_{12}\Phi_{1\theta}-A_{22}\Phi_{1r}}{A_{21}A_{12}-A_{22}A_{11}},$$

$$U_{46}=\frac{2B_{11}A_{22}+2A_{12}\left(-B_{21}-B_{22}\right)+2B_{12}A_{22}}{a\left(-2A_{11}A_{22}+2A_{12}A_{21}\right)}.$$

The potential energy equation of the structure is represented by

$$\begin{aligned}U=&\pi\int_0^a\Big[\left(N_r\varepsilon_r^0+M_r\chi_r\right)+\left(N_\theta\varepsilon_\theta^0+M_\theta\chi_\theta\right)\\&+Q_r\left(\psi+w_{,r}\right)\Big]rdr-\Bigg\{2\pi\int_0^a qwrdr-\\&-\pi\int_0^a\left[K_1wK_2\left(w_{,rr}+\frac{1}{r}w_{,r}\right)+K_3w^3\right]wrdr\Bigg\}-\\&\Delta T\pi\int_0^a\left(\Phi_{1r}\varepsilon_r^0+\Phi_{2r}\chi_r+\Phi_{1\theta}\varepsilon_\theta^0+\Phi_{2\theta}\chi_\theta\right)rdr.\end{aligned}\qquad(26)$$

Substituting Eqs. (15), (16), (18), (22), (23), and (25) to the potential energy, finally, applying the Ritz method, as follows

$$\frac{\partial U_{Total}}{\partial\Psi}=0,\text{ and }\frac{\partial U_{Total}}{\partial W}=0.\qquad(27)$$

The expression Ψ can be solved from the first expression of Eq. (27), as

$$\Psi=-M_1W^2+M_2WW^*+M_3W+M_4\Delta T.\qquad(28)$$

where the coefficients $M_i\left(i=1,...,4\right)$ are presented in Appendix.

Substituting Eq. (28) into the second expression of Eq. (27) yields the equation of the relationship between the loads and the deflection amplitude as follows

$$\begin{aligned}&\left(C_1-N_1K_3\right)W^3+\left(C_2W^*+C_3\right)W^2\\&+\left[C_4\left(W^*\right)^2+C_5W^*+C_6\Delta T+C_7-N_2K_1\right.\\&\left.-N_3K_2\right]W+C_8\Delta TW^*+C_9\Delta T-N_4q=0.\end{aligned}\qquad(29)$$

Eq. (29) is used to analyze the nonlinear thermo-mechanical buckling behavior of Pr-FG-GPLRC shallow spherical caps and circular plates. The post-buckling curves $W/h-q$ and $W/h-\Delta T$ are derived from Eq. (29)

$$\begin{aligned}q=\frac{1}{N_4}\Big[&\left(C_1-K_3N_1\right)W^3+\left(C_2W^*+C_3\right)W^2\\&+\left(C_4\left(W^*\right)^2+C_5W^*+C_6\Delta T+C_7\right.\\&\left.-K_1N_2-K_2N_3\right)W+C_8\Delta TW^*+C_9\Delta T\Big],\end{aligned}\qquad(30)$$

$$\begin{aligned}\Delta T=-\frac{1}{C_6W+C_8W^*+C_9}\Big[&\left(C_1-K_3N_1\right)W^3\\&+\left(C_2W^*+C_3\right)W^2+\left(C_4\left(W^*\right)^2+C_5W^*\right.\\&\left.+C_7-K_1N_2-K_2N_3\right)W-N_4q\Big].\end{aligned}\qquad(31)$$

where the coefficients $C_j\left(j=1,...,9\right)$ and $N_k\left(k=1,...,4\right)$ are presented in Appendix.

The thermal critical buckling loads of perfect circular plates $\left(W^*=0,R\to\infty\right)$ are obtained by applying $W\to0$ in Eq. (31)

$$\Delta T_{cr}=-\frac{C_7-K_1N_2-K_2N_3}{C_6}.\qquad(32)$$

4. Numerical examples

Table 1 illustrates the comparison of the thermal critical buckling loads $\Delta T_{cr}(K)$ of the perfect sandwich FG-GPLRC CPs with different coefficients of porosity in the study of Nam et al. [25] with the results of the present method. The results clearly show that the reliability of the present method is confirmed.

The numerical investigation is carried out to evaluate the thermo-mechanical behavior of Pr-FG-GPLRC CPs and SCs with different geometrical and foundation parameters. The Pr-FG-GPLRC is composed of copper matrix and GPLs frame with parameters taken from Wang et al. [26].

The critical thermal buckling load of perfect Pr-FG-GPLRC circular plates is investigated in Table 2. The effects of material parameters including foam coefficient, GPLs mass fraction, and foam distribution type are considered. The investigation results clearly show that when the foam coefficient increases, the critical thermal buckling load of PF-O circular plates increases, on the contrary, the critical thermal buckling load of PF-X circular plates decreases. In particular, the critical thermal buckling load of PF-U circular plates remains almost unchanged with increasing foam coefficient. With the same foam coefficient value, the mass fraction of GPLs increases, causing the critical thermal buckling load of three types of circular plates to increase. The foam coefficient and mass fraction of GPLs are taken as the same values to compare the thermal buckling load of circular plates with three different foam distributions. The PF-O distribution type showed the highest value, while the PF-X showed the lowest value.

Figs. 2a, and b show the comparison of the thermo-mechanical buckling curves of different spherical caps by three types of foam distributions, PF-O, PF-X, and PF-U. The results show that the curve of the PF-O foam distribution type is the highest and that of the PF-X foam distribution type is the lowest. However, the difference between the curves is clearly shown in the case of $q - W/h$ and is insignificant in the case of $\Delta T - W/h$. The influence of foam coefficient on the thermo-mechanical post-buckling curves of the Pr-FG-GPLRC spherical caps is investigated in Figs. 2c and d. It can be observed that the increase of foam coefficient causes the $q - W/h$ curves to be lowered, whereas the $\Delta T - W/h$ curves are raised. For both cases, the mechanical and thermal load capacity after buckling of the Pr-FG-GPLRC spherical caps increases sharply as the mass fraction of GPLs increases (Figs. 2e and f).

The geometric ratio a/h shows a large influence on the post-buckling mechanical load capacity of the spherical cap in Fig. 3a. The values of the geometric ratio a/h and the post-buckling mechanical load capacity of the spherical cap are opposite. The effect of imperfections on the post-buckling curves of the spherical caps is studied in Fig. 3b. In the small deflection region, the $q - W/h$ curves are lower with larger imperfections and this order is reversed in the large deflection region after passing through an intersection point of these curves.

The remarkable effects of the foundation parameters on the post-buckling mechanical and thermal behavior of the Pr-FG-GPLRC spherical caps can be obtained in Fig. 4. As the linear foundation parameters increase, both the $q - W/h$ and $\Delta T - W/h$ curves of the spherical caps are raised higher. Another important observation obtained in Fig. 4a is that increasing the linear foundation parameters also clearly reduces the snap-through phenomenon. In addition, the influence of nonlinear foundation parameters is considered in Figs. 4c and d for the cases of hard and soft foundations. It is clear that a steady upward trend is shown in the post-buckling curves for hard foundations. In contrast, a steady downward trend is shown in the post-buckling curves for soft foundations.

Table 1. Comparison of the critical thermal buckling loads $\Delta T_{cr}(K)$ of the perfect sandwich FG-GPLRC CPs (UD-PC-UD) with other results [25]

$$\left(\begin{array}{c} h=0.027m, a=35h, q=0MPa, K_1=8MN/m^3, K_2=0.2MN/m, K_3=0MN/m^5, \\ R=\infty, W^*=0, W^*_{GPL}=2\% \end{array}\right)$$

e_0	Present	Nam et al. [25]	Deviation (%)
0.2	68.9535	69.3236	0.5367
0.4	72.0065	72.5838	0.8017
0.6	74.2311	75.3874	1.5577
0.8	76.7919	77.5883	2.3701

Table 2. Effects of foam coefficient, GPLs mass fraction, and foam distribution type on the critical thermal buckling load $\Delta T_{cr}(K)$ of perfect Pr-FG-GPLRC CPs

$$\left(h=0.015m, a=35h, q=0MPa, K_1=0MN/m^3, K_2=0MN/m, K_3=0MN/m^5, R=\infty, W^*=0\right)$$

e_O	$W_{Gr}(\%)$	PF-U	PF-X	PF-O
0.1	2	25.43818927	24.14717231	26.18305686
	4	28.09727090	26.67116372	28.92014047
	6	30.61747114	29.06350250	31.51399238
0.3	2	25.43820709	21.10673482	28.02415919
	4	28.09733677	23.31263916	30.95361612
	6	30.61754302	25.40359851	33.73020175
0.5	2	25.43807384	17.40913970	30.55177877
	4	28.09729979	19.22865662	33.74587558
	6	30.61741646	20.95280862	36.77294942

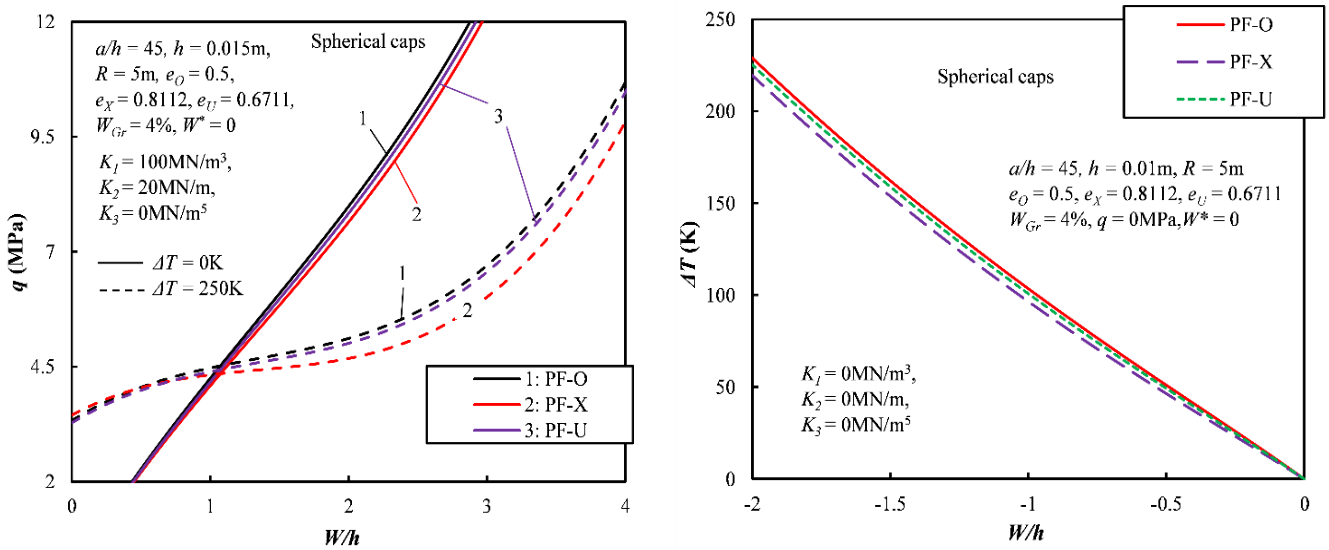

(a) (b)

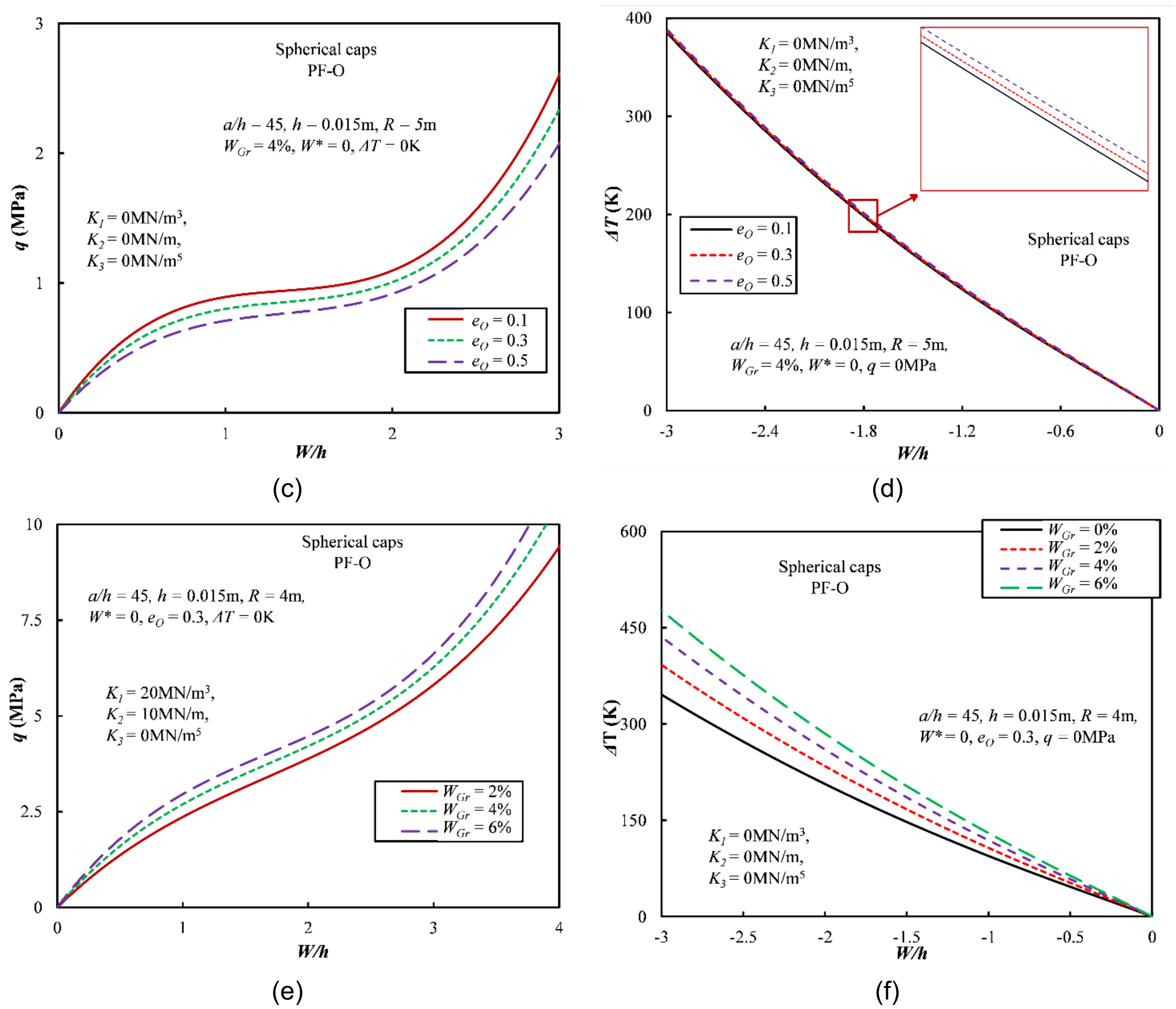

Fig. 2. Effects of material properties on the thermo-mechanical post-buckling curves of Pr-FG-GPLRC SCs

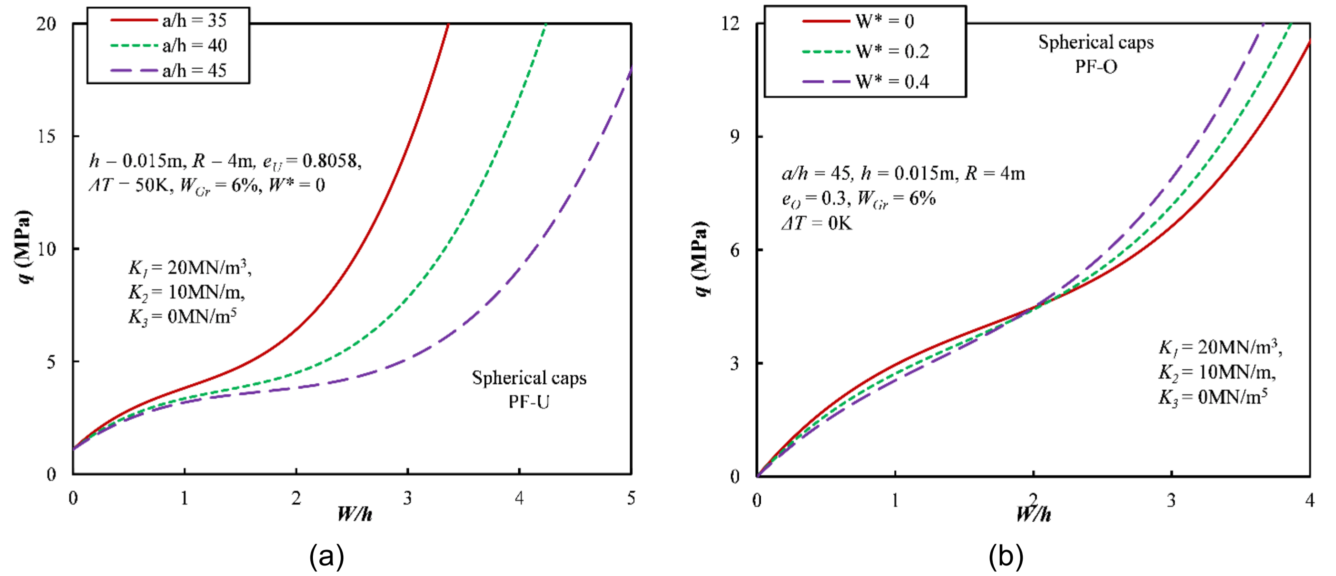

Fig. 3. Effects of geometrical properties on the mechanical post-buckling curves of Pr-FG-GPLRC SCs

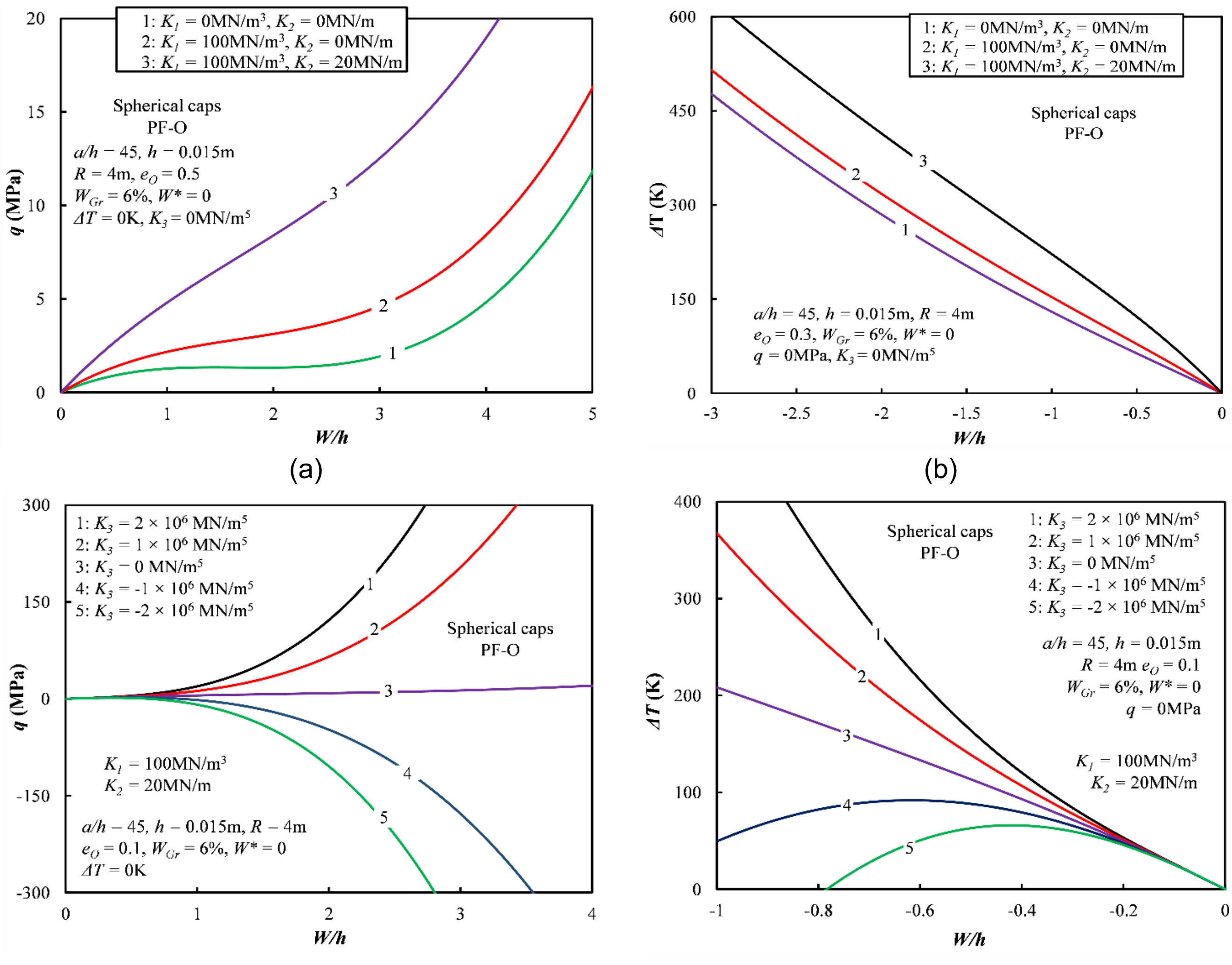

Fig. 4. Effects of foundation parameters on the thermo-mechanical post-buckling curves of Pr-FG-GPLRC SCs

5. Concluding remarks

This paper presents the analysis of the buckling and post-buckling behavior of Pr-FG-GPLRC circular plate and spherical cap structures subjected to external pressure loads and thermal loads distributed uniformly along the thickness of the shell. With the approach from the stress function, according to FSDT, the Rizt method is used. Some important results are as follows.

1) The post-buckling load capacity increases significantly and the snap-through strength decreases significantly as the mass fraction of GPLs increases.
2) The post-buckling load capacity of the PF-O spherical cap is the highest, while that of the PF-X spherical cap is the lowest.
3) The post-buckling curve of Pr-FG-GPLRC circular plates and spherical caps increases and the snap-through phenomenon decreases as the stiffness of the elastic foundation increases.

References

[1] R. Shahsiah, M.R. Eslami, R. Naj. (2006). Thermal Instability of Functionally Graded Shallow Spherical Shell. *Journal of Thermal. Stresses*, 29(8), 771-790.
[2] M.S. Boroujerdy, M.R. Eslami. (2013). Nonlinear axisymmetric thermomechanical response of piezo-FGM shallow spherical shells. *Archive of Applied Mechanics*, 83, 1681-1693.
[3] M.S. Boroujerdy, M.R. Eslami. (2014).

Axisymmetric snap-through behavior of Piezo-FGM shallow clamped spherical shells under thermo-electro-mechanical loading. *International Journal of Pressure Vessels and Piping*, 120-121, 19-26.

[4] A. Moosaie, H. Panahi-Kalus. (2017). Thermal stresses in an incompressible FGM spherical shell with temperature-dependent material properties. *Thin-Walled Structures*, 120, 215-224.

[5] N.T. Phuong, V.H. Nam, D.T. Dong. (2018). Nonlinear vibration of functionally graded sandwich shallow spherical caps resting on elastic foundations by using first-order shear deformation theory in thermal environment. *Journal of Sandwich Structures & Materials*, 22(4), 1157-1183.

[6] N.D. Duc, V.T.T. Anh, P.H. Cong. (2014). Nonlinear axisymmetric response of FGM shallow spherical shells on elastic foundations under uniform external pressure and temperature. *European Journal of Mechanics - A/Solids*, 45, 80-89.

[7] D.H. Bich, H.V. Tung. (2011). Non-linear axisymmetric response of functionally graded shallow spherical shells under uniform external pressure including temperature effects. *International Journal of Non-Linear Mechanics*, 46(9), 1195-1204.

[8] H.V. Tung. (2014). Nonlinear thermomechanical stability of shear deformable FGM shallow spherical shells resting on elastic foundations with temperature dependent properties. *Composite Structures*, 114, 107-116.

[9] H.V. Tung. (2016). Nonlinear axisymmetric response of FGM shallow spherical shells with tangential edge constraints and resting on elastic foundations. *Composite Structures*, 149, 231-238.

[10] R. Gholami, R. Ansari. (2017). Large deflection geometrically nonlinear analysis of functionally graded multilayer graphene platelet-reinforced polymer composite rectangular plates. Composite Structures, 180, 760-771.

[11] R. Gholami, R. Ansari. (2019). Nonlinear stability and vibration of pre/post-buckled multilayer FG-GPLRPC rectangular plates. *Applied Mathematical Modelling*, 65, 627-660.

[12] K. Zhu, R. Zhong, Q. Wang, X. Shi, B. Wu. (2024). Stationary Stochastic Response Analysis of the FG-GPLRC Irregular Quadrilateral Plate Based on the Chebyshev–Ritz Method. *International Journal of Structural Stability and Dynamics*, 24(12), 2450126.

[13] M. Karimiasl, A. Alibeigloo. (2022). Nonlinear free and forced vibration analysis of sandwich cylindrical panel with auxetic core and GPLRC facing sheets in hygrothermal environment. *Thin-Walled Structures*, 175, 109164.

[14] H. R. Esmaeili, Y. Kiani, and Y. T. Beni. (2022). Vibration characteristics of composite doubly curved shells reinforced with graphene platelets with arbitrary edge supports. *Acta Mechanica*, 233, 665-683.

[15] M. Javani, Y. Kiani, M.R. Eslami. (2020). Thermal buckling of FG graphene platelet reinforced composite annular sector plates. *Thin-Walled Structures*, 148, 106589.

[16] Y. Wang, R. Zeng, M. Safarpour. (2022). Vibration analysis of FG-GPLRC annular plate in a thermal environment. *Mechanics Based Design of Structures and Machines*, 50(1), 352-370.

[17] L.N. Ly, B.T. Tu, D.T.N. Thu, D.T. Dong, V.M. Duc, N.T. Phuong. (2022). Nonlinear thermo-mechanical buckling and postbuckling of sandwich FG-GPLRC spherical caps and circular plates with porous core by using higher-order shear deformation theory. *Journal of Thermoplastic Composite Materials*, 36(10), 4083-4105.

[18] N.T. Phuong, D.T. Dong, B.T. Tu, V.M. Duc, L.N. Khuong, P.T. Hieu, V.H. Nam. (2023). Nonlinear thermo-mechanical axisymmetric stability of FG-GPLRC spherical shells and

circular plates resting on nonlinear elastic medium. Ships and Offshore Structures, 19(6), 820-830.

[19] V.H. Nam, T.Q. Minh, P.T. Hieu, V.T. Hung, B.T. Tu, N.T.T. Hoai, D.T. Dong. (2023). A new analytical approach for nonlinear thermo-mechanical postbuckling of FG-GPLRC circular plates and shallow spherical caps stiffened by spiderweb stiffeners. *Thin-Walled Structures*, 193, 111296.

[20] D. Liu, Y. Zhou, J. Zhu. (2021). On the free vibration and bending analysis of functionally graded nanocomposite spherical shells reinforced with graphene nanoplatelets: Three-dimensional elasticity solutions. *Engineering Structures*, 226, 111376.

[21] K.C. Sun, Y.X. Hao, W. Zhang, S.W. Yang, Y.T. Cao. (2024). Effect of Graphene Reinforcement on Free Vibration and Material Properties of the FG-GPLRC Porous Cantilever Torsional Plate. *International Journal of Structural Stability and Dynamics*, 24(04), 2450041.

[22] Z. Qin, G.S. Jung, M.J. Kang, M.J. Buehler. (2017). The mechanics and design of a lightweight three-dimensional graphene assembly. *Science Advances*, 3(1), e1601536.

[23] A. Nieto, B. Boesl, A. Agarwal. (2015). Multi-scale intrinsic deformation mechanisms of 3D graphene foam. *Carbon*, 85, 299-308.

[24] J. Zhu, Z. Wang, L. Zhang, H. Wu, L. Zhao, H. Zhang, H. Wu. (2024). Wave Propagation in the Semi-Infinite Functionally Graded Porous Plates Reinforced with Graphene Platelets. *International Journal of Structural Stability and Dynamics*, 24(21), 2450245.

[25] V.H. Nam, B.T. Tu, V.T. Hung, C.V. Doan, N.T. Phuong. (2024). Nonlinear thermomechanical buckling and postbuckling analysis of sandwich FG-GPLRC complexly curved caps and circular plates with porous core. Acta Mech, 236, 421-438.

[26] Y. Wang, R. Zeng, M. Safarpour. (2022). Vibration analysis of FG-GPLRC annular plate in a thermal environment. Mechanics Based Design of Structures and Machines, 50(1), 352-370.

APPENDIX

$$
\begin{aligned}
M_1 = &-\frac{1}{6T_{19}U_{34}^2a^4 + \left(-12T_{17}U_{44}U_{34} + 24T_{19}U_{34}U_{46}\right)a^2 + 24T_{16}U_{44}^2 - 24T_{17}U_{44}U_{46} + 24T_{19}U_{46}^2}\Big[3T_{19}U_{11}U_{34}a^8 \\
&+\left(-3T_{17}U_{11}U_{44} + 6T_{19}U_{11}U_{46} + 4T_{19}U_{21}U_{34}\right)a^6 + \left(-4T_{17}U_{21}U_{44} + 8T_{19}U_{21}U_{46} + 6T_{19}U_{31}U_{34}\right)a^4 \\
&+\left(-6T_{17}U_{31}U_{44} + 12T_{19}U_{31}U_{46} + 12T_{19}U_{34}U_{41} - 6T_7U_{34}U_{44}\right)a^2 \\
&-12T_{17}U_{41}U_{44} + 24T_{19}U_{41}U_{46} + 12T_6U_{44}^2 - 12T_7U_{44}U_{46}\Big],
\end{aligned}
$$

$$
\begin{aligned}
M_2 = &-\frac{1}{6T_{19}U_{34}^2a^4 + \left(-12T_{17}U_{34}U_{44} + 24T_{19}U_{34}U_{46}\right)a^2 + 24T_{16}U_{44}^2 - 24T_{17}U_{44}U_{46} + 24T_{19}U_{46}^2}\Big[3a^8U_{34}U_{12}T_{19} \\
&+\left(-3T_{17}U_{12}U_{44} + 6T_{19}U_{12}U_{46} + 4T_{19}U_{22}U_{34}\right)a^6 + \left(-4T_{17}U_{22}U_{44} + 8T_{19}U_{22}U_{46} + 6T_{19}U_{32}U_{34}\right)a^4 \\
&+\left(-6T_{11}U_{34}U_{44} - 6T_{17}U_{32}U_{44} + 12T_{19}U_{32}U_{46} + 12T_{19}U_{34}U_{42}\right)a^2 \\
&+12T_{10}U_{44}^2 - 12T_{11}U_{44}U_{46} - 12T_{17}U_{42}U_{44} + 24U_{46}U_{42}T_{19}\Big],
\end{aligned}
$$

$$
\begin{aligned}
M_3 = &-\frac{1}{6T_{19}U_{34}^2a^4 + \left(-12T_{17}U_{44}U_{34} + 24T_{19}U_{34}U_{46}\right)a^2 + 24T_{16}U_{44}^2 - 24T_{17}U_{44}U_{46} + 24T_{19}U_{46}^2}\Big[4T_{19}U_{23}U_{34}a^6 \\
&+\left(-4T_{17}U_{23}U_{44} + 8T_{19}U_{23}U_{46} + 6T_{19}U_{33}U_{34}\right)a^4 + \left(-6T_{14}U_{34}U_{44} - 6T_{17}U_{33}U_{44} + 12T_{19}U_{33}U_{46} + 12T_{19}U_{34}U_{43}\right)a^2 \\
&+12T_{13}U_{44}^2 - 12T_{14}U_{44}U_{46} - 12T_{17}U_{43}U_{44} + 24T_{19}U_{43}U_{46}\Big],
\end{aligned}
$$

$$
M_4 = -\frac{\left(12T_{19}U_{34}U_{45} - 6T_{20}U_{34}U_{44}\right)a^2 - 12T_{17}U_{44}U_{45} + 12T_{18}U_{44}^2 + 24T_{19}U_{45}U_{46} - 12T_{20}U_{44}U_{46}}{6T_{19}U_{34}^2a^4 + \left(-12T_{17}U_{34}U_{44} + 24T_{19}U_{34}U_{46}\right)a^2 + 24T_{16}U_{44}^2 - 24T_{17}U_{44}U_{46} + 24T_{19}U_{46}^2},
$$

$$
\begin{aligned}
C_1 = &\frac{T_{19}a^{12}U_{11}^2}{4U_{44}^2} + \frac{2T_{19}U_{11}U_{21}a^{10}}{3U_{44}^2} + \frac{\left(6T_{19}\left(6M_1U_{34} + 6U_{31}\right)U_{11} + 32T_{19}U_{21}^2 + 3T_{19}U_{11}\left(12M_1U_{34} + 12U_{31}\right)\right)a^8}{72U_{44}^2} \\
&+\left(\begin{array}{l} \dfrac{6T_{19}\left(12M_1U_{46} + 12U_{41}\right)U_{11} + 8T_{19}\left(6M_1U_{34} + 6U_{31}\right)U_{21}}{72U_{44}^2} \\ + \dfrac{4T_{19}U_{21}\left(12M_1U_{34} + 12U_{31}\right) + 3T_{19}U_{11}\left(24M_1U_{46} + 24U_{41}\right)}{72U_{44}^2} - \dfrac{T_7U_{11} + T_{17}M_1U_{11}}{U_{44}} \end{array}\right)a^6 \\
&+\left(\begin{array}{l} \dfrac{8T_{19}\left(12M_1U_{46} + 12U_{41}\right)U_{21} + T_{19}\left(6M_1U_{34} + 6U_{31}\right)\left(12M_1U_{34} + 12U_{31}\right) + 4T_{19}U_{21}\left(24M_1U_{46} + 24U_{41}\right)}{72U_{44}^2} \\ - \dfrac{4T_7U_{21} + 4T_{17}M_1U_{21}}{3U_{44}} \end{array}\right)a^4 \\
&+\left(\begin{array}{l} \dfrac{T_{19}\left(12M_1U_{46} + 12U_{41}\right)\left(12M_1U_{34} + 12U_{31}\right) + T_{19}\left(6M_1U_{34} + 6U_{31}\right)\left(24M_1U_{46} + 24U_{41}\right)}{72U_{44}^2} \\ - \dfrac{\left(T_{17}M_1 + T_7\right)\left(6M_1U_{34} + 6U_{31}\right)}{6U_{44}} - \dfrac{\left(T_{17}M_1 + T_7\right)\left(12M_1U_{34} + 12U_{31}\right)}{12U_{44}} \end{array}\right)a^2 \\
&+\frac{T_{19}\left(12M_1U_{46} + 12U_{41}\right)\left(24M_1U_{46} + 24U_{41}\right)}{72U_{44}^2} - \frac{\left(T_{17}M_1 + T_7\right)\left(12M_1U_{46} + 12U_{41}\right)}{6U_{44}} \\
&-\frac{\left(T_{17}M_1 + T_7\right)\left(24M_1U_{46} + 24U_{41}\right)}{12U_{44}} + 4T_{16}M_1^2 + 4T_6M_1 + 4T_1,
\end{aligned}
$$

$$\begin{aligned}
C_2 = {} & \frac{1}{24U_{44}^2}\Big[9T_{19}U_{11}U_{12}a^{12} + 12T_{19}\left(U_{11}U_{22}+U_{12}U_{21}\right)a^{10} \\
& +18\left(U_{11}U_{34}M_2 + U_{12}U_{34}M_1 + U_{11}U_{32} + U_{12}U_{31} + \frac{8}{9}U_{21}U_{22}\right)T_{19}a^8 \\
& +\begin{pmatrix} T_{19}\left(36U_{12}U_{46}+24U_{22}U_{34}\right)M_1 + T_{19}\left(36U_{11}U_{46}+24U_{21}U_{34}\right)M_2 \\ +\left(36U_{11}U_{42}+36U_{12}U_{41}+24U_{21}U_{32}+24U_{22}U_{31}\right)T_{19} \\ -18U_{44}\left(M_1T_{17}U_{12}+M_2T_{17}U_{11}+T_{11}U_{11}+T_7U_{12}\right)\end{pmatrix}a^6 \\
& +\begin{pmatrix}\left(36M_2U_{34}^2+48U_{22}U_{46}+36U_{32}U_{34}\right)T_{19}M_1 + \left(48U_{21}U_{46}+36U_{31}U_{34}\right)T_{19}M_2 \\ +\left(48U_{21}U_{42}+48U_{22}U_{41}+36U_{31}U_{32}\right)T_{19} - 24U_{44}\left(M_1T_{17}U_{22}+M_2T_{17}U_{21}+T_{11}U_{21}+T_7U_{22}\right)\end{pmatrix}a^4 \\
& +\begin{pmatrix}\begin{pmatrix}\left(144M_2U_{34}U_{46}+72U_{32}U_{46}+72U_{34}U_{42}\right)M_1 \\ +\left(72U_{31}U_{46}+72U_{34}U_{41}\right)M_2 + 72U_{31}U_{42}+72U_{32}U_{41}\end{pmatrix}T_{19} \\ -36U_{44}\left(\left(2M_2T_{17}U_{34}+T_{11}U_{34}+T_{17}U_{32}\right)M_1 + \left(T_{17}U_{31}+T_7U_{34}\right)M_2 + U_{31}T_{11}+U_{32}T_7\right)\end{pmatrix}a^2 \\
& +144\left(M_2U_{46}+U_{42}\right)\left(M_1U_{46}+U_{41}\right)T_{19} - 72U_{44}^2\left(\left(-2M_2T_{16}-T_{10}\right)M_1 - T_6M_2 - T_2\right) \\
& -72U_{44}\left(\left(2M_2T_{17}U_{46}+T_{11}U_{46}+T_{17}U_{42}\right)M_1 + \left(T_{17}U_{41}+T_7U_{46}\right)M_2 + U_{41}T_{11}+U_{42}T_7\right)\Big],
\end{aligned}$$

$$\begin{aligned}
C_3 = {} & \frac{1}{12U_{44}^2}\Big[6T_{19}U_{11}U_{23}a^{10} + 9\left(U_{11}U_{34}M_3+U_{11}U_{33}+\frac{8}{9}U_{21}U_{23}\right)T_{19}a^8 \\
& +\begin{pmatrix}\left(\left(18U_{11}U_{46}+12U_{21}U_{34}\right)M_3 + 12U_{23}U_{34}M_1 + 18U_{11}U_{43}+12U_{21}U_{33}+12U_{23}U_{31}\right)T_{19} \\ -9U_{11}U_{44}\left(M_3T_{17}+T_{14}\right)\end{pmatrix}a^6 \\
& +\begin{pmatrix}\begin{pmatrix}\left(18M_1U_{34}^2+24U_{21}U_{46}+18U_{31}U_{34}\right)M_3 \\ +\left(24U_{23}U_{46}+18U_{33}U_{34}\right)M_1 + 24U_{21}U_{43}+24U_{23}U_{41}+18U_{31}U_{33}\end{pmatrix}T_{19} \\ -12U_{44}\left(M_1T_{17}U_{23}+M_3T_{17}U_{21}+T_{14}U_{21}+T_7U_{23}\right)\end{pmatrix}a^4 \\
& +\begin{pmatrix}\begin{pmatrix}\left(72M_1U_{34}U_{46}+36U_{31}U_{46}+36U_{34}U_{41}\right)M_3 \\ +\left(36U_{33}U_{46}+36U_{34}U_{43}\right)M_1+36U_{31}U_{43}+36U_{41}U_{33}\end{pmatrix}T_{19} \\ -18U_{44}\left(\left(2M_1T_{17}U_{34}+T_{17}U_{31}+T_7U_{34}\right)M_3 + \left(T_{14}U_{34}+T_{17}U_{33}\right)M_1 + U_{31}T_{14}+T_7U_{33}\right)\end{pmatrix}a^2 \\
& +72\left(M_3U_{46}+U_{43}\right)\left(M_1U_{46}+U_{41}\right)T_{19} \\
& -36U_{44}\begin{pmatrix}\left(\left(-2M_1T_{16}-T_6\right)M_3 - T_{13}M_1 - T_3\right)U_{44} + \left(2M_1T_{17}U_{46}+T_{17}U_{41}+T_7U_{46}\right)M_3 \\ +\left(T_{14}U_{46}+T_{17}U_{43}\right)M_1 + U_{41}T_{14}+T_7U_{43}\end{pmatrix}\Big],
\end{aligned}$$

$$\begin{aligned}
C_4 = {} & \frac{1}{72U_{44}^2}\Big[9T_{19}U_{12}^2a^{12} + 24T_{19}U_{12}U_{22}a^{10} + 16T_{19}\left(\frac{9}{4}U_{34}M_2U_{12} + U_{22}^2 + \frac{9}{4}U_{32}U_{12}\right)a^8 \\
& +\left(\left(\left(72U_{12}U_{46}+48U_{34}U_{22}\right)M_2 + 48U_{22}U_{32}+72U_{42}U_{12}\right)T_{19} - 36U_{44}U_{12}\left(T_{17}M_2+T_{11}\right)\right)a^6 \\
& +\left(\left(36U_{34}^2M_2^2 + \left(96U_{22}U_{46}+72U_{32}U_{34}\right)M_2 + 96U_{22}U_{42}+36U_{32}^2\right)T_{19} - 48U_{22}U_{44}\left(T_{17}M_2+T_{11}\right)\right)a^4 \\
& +144\left(M_2U_{34}+U_{32}\right)\left(\left(M_2U_{46}+U_{42}\right)T_{19} - \frac{U_{44}\left(T_{17}M_2+T_{11}\right)}{2}\right)a^2 + 144\left(M_2U_{46}+U_{42}\right)^2T_{19} \\
& -144U_{44}\left(\left(-T_{16}U_{44}+T_{17}U_{46}\right)M_2^2 + \left(-T_{10}U_{44}+T_{11}U_{46}+T_{17}U_{42}\right)M_2 + U_{42}T_{11} - T_4U_{44}\right)\Big],
\end{aligned}$$

$$
\begin{aligned}
C_5 = \frac{1}{18U_{44}^2}\Bigg[& 6T_{19}U_{12}U_{23}a^{10} + 9\left(U_{12}U_{34}M_3 + U_{12}U_{33} + \frac{8}{9}U_{22}U_{23}\right)T_{19}a^8 \\
& + \left(\begin{array}{l} \left(\left(18U_{12}U_{46} + 12U_{22}U_{34}\right)M_3 + 12U_{23}U_{34}M_2 + 18U_{12}U_{43} + 12U_{22}U_{33} + 12U_{23}U_{32}\right)T_{19} \\ -9U_{12}U_{44}\left(T_{17}M_3 + T_{14}\right) \end{array}\right)a^6 \\
& + \left(\begin{array}{l} \left(\begin{array}{l} \left(18M_2U_{34}^2 + 24U_{22}U_{46} + 18U_{32}U_{34}\right)M_3 + \left(24U_{23}U_{46} + 18U_{33}U_{34}\right)M_2 \\ +24U_{22}U_{43} + 24U_{23}U_{42} + 18U_{32}U_{33} \end{array}\right)T_{19} \\ -12U_{44}\left(T_{17}M_2U_{23} + T_{17}M_3U_{22} + T_{11}U_{23} + T_{14}U_{22}\right) \end{array}\right)a^4 \\
& + \left(\begin{array}{l} \left(\begin{array}{l} \left(72M_2U_{34}U_{46} + 36U_{32}U_{46} + 36U_{34}U_{42}\right)M_3 + \left(36U_{33}U_{46} + 36U_{34}U_{43}\right)M_2 \\ +36U_{32}U_{43} + 36U_{42}U_{33} \end{array}\right)T_{19} \\ -18U_{44}\left(\left(2M_2T_{17}U_{34} + T_{11}U_{34} + T_{17}U_{32}\right)M_3 + \left(T_{14}U_{34} + T_{17}U_{33}\right)M_2 + U_{32}T_{14} + T_{11}U_{33}\right) \end{array}\right)a^2 \\
& + 72\left(M_3U_{46} + U_{43}\right)\left(M_2U_{46} + U_{42}\right)T_{19} \\
& - 36U_{44}\left(\begin{array}{l} \left(\left(-2M_2T_{16} - T_{10}\right)M_3 - T_{13}M_2 - T_5\right)U_{44} + \left(2M_2T_{17}U_{46} + T_{11}U_{46} + T_{17}U_{42}\right)M_3 \\ +\left(T_{14}U_{46} + T_{17}U_{43}\right)M_2 + U_{42}T_{14} + T_{11}U_{43} \end{array}\right)\Bigg],
\end{aligned}
$$

$$
\begin{aligned}
C_6 = \frac{1}{6U_{44}^2}\Bigg[& 3M_4T_{19}U_{11}U_{34}a^8 + \left(-3U_{11}\left(T_{17}M_4 + T_{20}\right)U_{44} + 6T_{19}\left(\left(U_{11}U_{46} + \frac{2U_{21}U_{34}}{3}\right)M_4 + U_{11}U_{45}\right)\right)a^6 \\
& + \left(-4U_{21}\left(T_{17}M_4 + T_{20}\right)U_{44} + 8T_{19}\left(\left(\frac{3}{4}U_{34}^2M_1 + U_{21}U_{46} + \frac{3}{4}U_{31}U_{34}\right)M_4 + U_{21}U_{45}\right)\right)a^4 \\
& + \left(\begin{array}{l} \left(\left(-12M_1T_{17}U_{34} - 6T_{17}U_{31} - 6T_7U_{34}\right)M_4 - 6T_{20}\left(M_1U_{34} + U_{31}\right)\right)U_{44} \\ +12T_{19}\left(\left(2M_1U_{34}U_{46} + U_{31}U_{46} + U_{34}U_{41}\right)M_4 + U_{45}\left(M_1U_{34} + U_{31}\right)\right) \end{array}\right)a^2 \\
& + \left(\left(24M_1T_{16} + 12T_6\right)M_4 + 12T_{18}M_1 + 12T_8\right)U_{44}^2 + 24T_{19}\left(M_4U_{46} + U_{45}\right)\left(M_1U_{46} + U_{41}\right) \\
& + \left(\left(-24M_1T_{17}U_{46} - 12T_{17}U_{41} - 12T_7U_{46}\right)M_4 + \left(-12T_{17}U_{45} - 12T_{20}U_{46}\right)M_1 - 12T_{20}U_{41} - 12T_7U_{45}\right)U_{44}\Bigg],
\end{aligned}
$$

$$
\begin{aligned}
C_7 = & \frac{2T_{19}U_{23}^2a^8}{9U_{44}^2} + \frac{\left(12U_{34}T_{19}U_{23}M_3 + 12T_{19}U_{23}U_{33}\right)a^6}{18U_{44}^2} + \frac{36T_{19}U_{43}^2 - 36T_{14}U_{43}U_{44} + 36T_9U_{44}^2}{18U_{44}^2} \\
& + \frac{\left(9M_3^2T_{19}U_{34}^2 + \left(\left(24U_{23}U_{46} + 18U_{33}U_{34}\right)T_{19} - 12U_{44}T_{17}U_{23}\right)M_3 + \left(24U_{23}U_{43} + 9U_{33}^2\right)T_{19} - 12T_{14}U_{23}U_{44}\right)a^4}{18U_{44}^2} \\
& + \frac{\left(\begin{array}{l} -18U_{34}\left(T_{17}U_{44} - 2T_{19}U_{46}\right)M_3^2 + \left(\left(36U_{33}U_{46} + 36U_{34}U_{43}\right)T_{19} - 18U_{44}\left(T_{14}U_{34} + T_{17}U_{33}\right)\right)M_3 \\ +36U_{33}\left(U_{43}T_{19} - \frac{T_{14}U_{44}}{2}\right) \end{array}\right)a^2}{18U_{44}^2} \\
& + \frac{\left(36T_{16}U_{44}^2 - 36T_{17}U_{44}U_{46} + 36T_{19}U_{46}^2\right)M_3^2 + \left(72U_{43}U_{46}T_{19} - 36U_{44}\left(-T_{13}U_{44} + T_{14}U_{46} + T_{17}U_{43}\right)\right)M_3}{18U_{44}^2},
\end{aligned}
$$

$$C_8=\frac{T_{19}M_4U_{34}U_{12}a^8}{4U_{44}^2}+\frac{\left(-3U_{12}\left(M_4T_{17}+T_{20}\right)U_{44}+6\left(\left(U_{12}U_{46}+\frac{2U_{22}U_{34}}{3}\right)M_4+U_{12}U_{45}\right)T_{19}\right)a^6}{12U_{44}^2}$$

$$+\frac{\left(-4U_{22}\left(M_4T_{17}+T_{20}\right)U_{44}+8\left(\left(\frac{3}{4}U_{34}^2M_2+U_{22}U_{46}+\frac{3}{4}U_{32}U_{34}\right)M_4+U_{22}U_{45}\right)T_{19}\right)a^4}{12U_{44}^2}$$

$$+\frac{1}{12U_{44}^2}\begin{pmatrix}\left(\left(-12M_2T_{17}U_{34}-6T_{11}U_{34}-6T_{17}U_{32}\right)M_4-6T_{20}\left(M_2U_{34}+U_{32}\right)\right)U_{44}\\+12\left(\left(2M_2U_{34}U_{46}+U_{32}U_{46}+U_{34}U_{42}\right)M_4+U_{45}\left(M_2U_{34}+U_{32}\right)\right)T_{19}\end{pmatrix}a^2$$

$$+\frac{\left(-24M_2T_{17}U_{46}-12T_{11}U_{46}-12T_{17}U_{42}\right)M_4+\left(-12T_{17}U_{45}-12T_{20}U_{46}\right)M_2-12T_{20}U_{42}-12T_{11}U_{45}}{12U_{44}}$$

$$+\frac{\left(24M_2T_{16}+12T_{10}\right)M_4+12T_{18}M_2+12T_{12}}{12}+\frac{24T_{19}\left(M_4U_{46}+U_{45}\right)\left(M_2U_{46}+U_{42}\right)}{12U_{44}^2},$$

$$C_9=\frac{T_{19}M_4U_{34}U_{23}a^6}{3U_{44}^2}$$

$$+\frac{\left(\left(-2T_{17}M_4U_{23}-2T_{20}U_{23}\right)U_{44}+2T_{19}\left(\frac{3U_{34}M_3}{2}+\frac{3U_{33}}{2}\right)M_4U_{34}+2T_{19}U_{23}\left(2M_4U_{46}+2U_{45}\right)\right)a^4}{6U_{44}^2}$$

$$+\frac{1}{6U_{44}^2}\begin{pmatrix}\left(\left(-6M_3T_{17}U_{34}-3T_{14}U_{34}-3T_{17}U_{33}\right)M_4-3T_{20}\left(U_{34}M_3+U_{33}\right)\right)U_{44}\\+2T_{19}\left(3M_3U_{46}+3U_{43}\right)M_4U_{34}+2T_{19}\left(\frac{3U_{34}M_3}{2}+\frac{3U_{33}}{2}\right)\left(2M_4U_{46}+2U_{45}\right)\end{pmatrix}a^2$$

$$+\frac{\left(12M_3T_{16}+6T_{13}\right)M_4+6T_{18}M_3+6T_{15}}{6}+\frac{2T_{19}\left(3M_3U_{46}+3U_{43}\right)\left(2M_4U_{46}+2U_{45}\right)}{6U_{44}^2}$$

$$+\frac{\left(-12U_{46}M_3T_{17}-6U_{46}T_{14}-6U_{43}T_{17}\right)M_4+\left(-6T_{17}U_{45}-6T_{20}U_{46}\right)M_3-6T_{20}U_{43}-6T_{14}U_{45}}{6U_{44}},$$

$$G_{111}=Y_{11}^2\left(7A_{21}^*+7A_{12}^*+49A_{22}^*+A_{11}^*\right),\quad G_{112}=2Y_{11}Y_{12}\left(7A_{21}^*+7A_{12}^*+49A_{22}^*+A_{11}^*\right),$$

$$G_{113}=Y_{12}^2\left(7A_{21}^*+7A_{12}^*+49A_{22}^*+A_{11}^*\right),\quad G_{121}=2Y_{11}Y_{21}\left(6A_{21}^*+6A_{12}^*+35A_{22}^*+A_{11}^*\right),$$

$$G_{122}=2\left(Y_{11}Y_{22}+Y_{12}Y_{21}\right)\left(6A_{21}^*+6A_{12}^*+35A_{22}^*+A_{11}^*\right),\ G_{123}=2Y_{11}Y_{23}\left(6A_{21}^*+6A_{12}^*+35A_{22}^*+A_{11}^*\right),$$

$$G_{124}=2Y_{12}Y_{22}\left(6A_{21}^*+6A_{12}^*+35A_{22}^*+A_{11}^*\right),\ G_{125}=2Y_{12}Y_{23}\left(6A_{21}^*+6A_{12}^*+35A_{22}^*+A_{11}^*\right),$$

$$G_{131}=2Y_{31}Y_{11}\left(5A_{21}^*+5A_{12}^*+21A_{22}^*+A_{11}^*\right)+Y_{21}^2\left(5A_{21}^*+5A_{12}^*+25A_{22}^*+A_{11}^*\right),$$

$$G_{132}=\left(42Y_{32}Y_{11}+42Y_{31}Y_{12}\right)\left(\frac{5A_{21}^*+5A_{12}^*+A_{11}^*}{21}+A_{22}^*\right)$$

$$+50Y_{21}Y_{22}\left(\frac{A_{21}^*+A_{12}^*}{5}+\frac{A_{11}^*}{25}+A_{22}^*\right),$$

$$G_{133}=2Y_{33}Y_{11}\left(5A_{21}^*+5A_{12}^*+21A_{22}^*+A_{11}^*\right)+2Y_{21}Y_{23}\left(5A_{21}^*+5A_{12}^*++25A_{22}^*+A_{11}^*\right),$$

$$G_{134}=2Y_{32}Y_{12}\left(5A_{21}^*+5A_{12}^*+21A_{22}^*+A_{11}^*\right)+Y_{22}^2\left(5A_{21}^*+5A_{12}^*+25A_{22}^*+A_{11}^*\right),$$

$$G_{135}=2Y_{33}Y_{12}\left(5A_{21}^{*}+5A_{12}^{*}+21A_{22}^{*}+A_{11}^{*}\right)+2Y_{22}Y_{23}\left(5A_{21}^{*}+5A_{12}^{*}+25A_{22}^{*}+A_{11}^{*}\right),$$

$$G_{136}=-\frac{Y_{11}}{a^{3}}\left(21B_{21}^{*}+B_{12}^{*}+C_{21}^{*}+21C_{12}^{*}+7B_{22}^{*}+7C_{22}^{*}+3C_{11}^{*}+3B_{11}^{*}\right),$$

$$G_{137}=Y_{23}^{2}\left(+5A_{21}^{*}+5A_{12}^{*}+25A_{22}^{*}+A_{11}^{*}\right),$$

$$G_{138}=-\frac{Y_{12}}{a^{3}}\left(3B_{11}^{*}+B_{12}^{*}+3C_{11}^{*}+21C_{12}^{*}+21B_{21}^{*}+7B_{22}^{*}+C_{21}^{*}+7C_{22}^{*}\right),$$

$$G_{141}=2Y_{51}Y_{11}\left(4A_{21}^{*}+4A_{12}^{*}+7A_{22}^{*}+A_{11}^{*}\right)+2Y_{21}Y_{31}\left(4A_{21}^{*}+4A_{12}^{*}+15A_{22}^{*}+A_{11}^{*}\right),$$

$$G_{142}=\left(2Y_{11}Y_{53}+2Y_{12}Y_{51}+2Y_{21}Y_{32}+2Y_{22}Y_{31}\right)A_{11}^{*}+\left(8Y_{11}Y_{53}+8Y_{12}Y_{51}+8Y_{21}Y_{32}+8Y_{22}Y_{31}\right)A_{12}^{*}$$
$$+\left(8Y_{11}Y_{53}+8Y_{12}Y_{51}+8Y_{21}Y_{32}+8Y_{22}Y_{31}\right)A_{21}^{*}+14\left(Y_{11}Y_{53}+Y_{12}Y_{51}+\frac{15Y_{21}Y_{32}}{7}+\frac{15Y_{22}Y_{31}}{7}\right)A_{22}^{*},$$

$$G_{143}=14Y_{52}Y_{11}\left(A_{22}^{*}+\frac{4A_{21}^{*}+4A_{12}^{*}+A_{11}^{*}}{7}\right)+30\left(Y_{21}Y_{33}+Y_{23}Y_{31}\right)\left(A_{22}^{*}+\frac{4A_{21}^{*}+A_{11}^{*}+4A_{12}^{*}}{15}\right),$$

$$G_{144}=2Y_{53}Y_{12}\left(4A_{21}^{*}+4A_{12}^{*}+7A_{22}^{*}+A_{11}^{*}\right)+2Y_{22}Y_{32}\left(4A_{21}^{*}+4A_{12}^{*}+15A_{22}^{*}+A_{11}^{*}\right),$$

$$G_{145}=14Y_{52}Y_{12}\left(\frac{7A_{22}^{*}+4A_{21}^{*}+A_{11}^{*}+4A_{12}^{*}}{7}\right)+30\left(Y_{22}Y_{33}+Y_{23}Y_{32}\right)\left(\frac{4A_{12}^{*}+4A_{21}^{*}+15A_{22}^{*}+A_{11}^{*}}{15}\right),$$

$$G_{146}=\frac{1}{a^{3}}\Big[Y_{11}\left(7B_{22}^{*}+C_{21}^{*}+7C_{22}^{*}+B_{12}^{*}+7B_{21}^{*}+C_{11}^{*}+B_{11}^{*}+7C_{12}^{*}\right)a^{2}$$
$$-Y_{21}\left(15C_{12}^{*}+5C_{22}^{*}+C_{21}^{*}+B_{12}^{*}+3B_{11}^{*}+15B_{21}^{*}+5B_{22}^{*}+3C_{11}^{*}\right)\Big],$$

$$G_{147}=-Y_{11}\left(\Phi_{1r}^{*}+7\Phi_{1\theta}^{*}\right),\quad G_{148}=2Y_{11}\left(A_{11}^{*}+4A_{12}^{*}+4A_{21}^{*}+7A_{22}^{*}\right),$$

$$G_{149}=2Y_{23}Y_{33}\left(A_{11}^{*}+4A_{12}^{*}+4A_{21}^{*}+15A_{22}^{*}\right)+\frac{16K_{s}H_{44}}{a^{8}},$$

$$G_{1410}=\frac{Y_{12}}{a}\left(C_{21}^{*}+B_{12}^{*}+B_{11}^{*}+7B_{21}^{*}+7B_{22}^{*}+C_{11}^{*}+7C_{12}^{*}+7C_{22}^{*}\right)$$
$$-\frac{Y_{12}Y_{22}}{a^{3}}\left(C_{21}^{*}+5C_{22}^{*}+3B_{11}^{*}+B_{12}^{*}+15B_{21}^{*}+5B_{22}^{*}+15C_{12}^{*}+3C_{11}^{*}\right),$$

$$G_{1411}=-Y_{12}\left(\Phi_{1r}^{*}+7\Phi_{1\theta}^{*}\right),\quad G_{1412}=2Y_{12}\left(A_{11}^{*}+4A_{12}^{*}+4A_{21}^{*}+7A_{22}^{*}\right),$$

$$G_{1413}=\frac{-15Y_{23}}{a^{3}}\left(C_{12}^{*}+\frac{C_{21}^{*}+B_{12}^{*}}{15}+\frac{C_{22}^{*}+B_{22}^{*}}{3}+\frac{C_{11}^{*}+B_{11}^{*}}{5}+B_{21}^{*}\right)-\frac{8K_{s}H_{44}}{a^{7}},$$

$$G_{1414}=\frac{K_{s}H_{44}}{a^{6}},\quad G_{151}=2Y_{51}Y_{21}\left(3A_{21}^{*}+A_{11}^{*}+5A_{22}^{*}+3A_{12}^{*}\right)+Y_{31}^{2}\left(+3A_{21}^{*}+3A_{12}^{*}+9A_{22}^{*}+A_{11}^{*}\right),$$

$$G_{152}=10Y_{53}Y_{21}\left(\frac{3A_{21}^{*}+A_{11}^{*}+3A_{12}^{*}}{5}+A_{22}^{*}\right)+10Y_{51}Y_{22}\left(\frac{3A_{21}^{*}+A_{11}^{*}+3A_{12}^{*}}{5}+A_{22}^{*}\right)$$
$$+18Y_{32}Y_{31}\left(\frac{3A_{21}^{*}+3A_{12}^{*}+A_{11}^{*}}{9}+A_{22}^{*}\right),$$

$$G_{153}=10Y_{52}Y_{21}\left(A_{22}^{*}+\frac{3A_{21}^{*}+3A_{12}^{*}+A_{11}^{*}}{5}\right)+10Y_{51}Y_{23}\left(A_{22}^{*}+\frac{3A_{21}^{*}+3A_{12}^{*}+A_{11}^{*}}{5}\right)$$
$$+18Y_{33}Y_{31}\left(A_{22}^{*}+\frac{3A_{21}^{*}+3A_{12}^{*}+A_{11}^{*}}{9}\right),$$

$$G_{154}=2Y_{53}Y_{22}\left(3A^*_{21}+5A^*_{22}+3A^*_{12}+A^*_{11}\right)+Y^2_{32}\left(3A^*_{21}+3A^*_{12}+9A^*_{22}+A^*_{11}\right),$$

$$G_{155}=\left(10Y_{52}Y_{22}+10Y_{53}Y_{23}\right)\left(\frac{3A^*_{21}+3A^*_{12}+A^*_{11}}{5}+A^*_{22}\right)$$
$$+18Y_{32}Y_{33}\left(\frac{3A^*_{21}+3A^*_{12}+A^*_{11}}{9}+A^*_{22}\right),$$

$$G_{156}=\frac{Y_{21}}{a}\left(C^*_{21}+B^*_{12}+5C^*_{22}+B^*_{11}+5B^*_{21}+5C^*_{12}+5B^*_{22}+C^*_{11}\right)$$
$$-\frac{Y_{31}}{a^3}\left(C^*_{21}+B^*_{12}+3C^*_{22}+3B^*_{11}+3C^*_{11}+9B^*_{21}+3B^*_{22}+9C^*_{12}\right),$$

$$G_{157}=-Y_{21}\left(\Phi^*_{1r}+5\Phi^*_{1\theta}\right),\qquad G_{158}=2Y_{21}\left(3A^*_{21}+3A^*_{12}+5A^*_{22}+A^*_{11}\right),$$

$$G_{159}=\frac{10Y_{52}Y_{23}\left(\frac{3A^*_{12}+3A^*_{21}+A^*_{11}}{5}+A^*_{22}\right)}{a^6}+9Y^2_{33}\left(A^*_{22}+\frac{A^*_{11}}{9}+\frac{A^*_{12}}{3}+\frac{A^*_{21}}{3}\right)-\frac{32K_sH_{44}}{a^6},$$

$$G_{1510}=\frac{Y_{22}}{a}\left(C^*_{21}+B^*_{12}+5C^*_{22}+5B^*_{21}+5B^*_{22}+5C^*_{12}+C^*_{11}+B^*_{11}\right)$$
$$-\frac{Y_{32}}{a^3}\left(B^*_{12}+C^*_{21}+3B^*_{11}+9B^*_{21}+3C^*_{11}+9C^*_{12}+3C^*_{22}+3B^*_{22}\right),$$

$$G_{1511}=-Y_{22}\left(\Phi^*_{1r}+5\Phi^*_{1\theta}\right),\quad G_{1512}=2Y_{22}\left(A^*_{11}+3A^*_{12}+3A^*_{21}+5A^*_{22}\right),$$

$$G_{1513}=2Y_{23}\left(A^*_{11}+3A^*_{12}+3A^*_{21}+5A^*_{22}\right),\quad G_{1514}=-Y_{23}\left(\Phi^*_{1r}+5\Phi^*_{1\theta}\right),$$

$$G_{1515}=\frac{Y_{23}}{a}\left(B^*_{12}+C^*_{11}+5C^*_{12}+C^*_{21}+5C^*_{22}+5B^*_{22}+B^*_{11}+5B^*_{21}\right)$$
$$-\frac{3Y_{33}}{a^3}\left(\frac{B^*_{12}}{3}+3C^*_{12}+C^*_{11}+\frac{C^*_{21}}{3}+B^*_{22}+C^*_{22}+B^*_{11}+3B^*_{21}\right)+\frac{16K_sH_{44}}{a^5},$$

$$G_{1516}=\frac{9D^*_{11}+3D^*_{12}+3D^*_{21}+D^*_{22}}{a^6}-\frac{2K_sH_{44}}{a^4},\ G_{161}=2Y_{31}Y_{51}\left(2A^*_{21}+2A^*_{12}+3A^*_{22}+A^*_{11}\right),$$

$$G_{162}=2\left(Y_{31}Y_{53}+Y_{32}Y_{51}\right)\left(2A^*_{21}+2A^*_{12}+3A^*_{22}+A^*_{11}\right),G_{163}=2\left(Y_{31}Y_{52}+Y_{33}Y_{51}\right)\left(2A^*_{21}+2A^*_{12}+3A^*_{22}+A^*_{11}\right),$$

$$G_{164}=2Y_{32}Y_{53}\left(2A^*_{21}+2A^*_{12}+3A^*_{22}+A^*_{11}\right),G_{165}=2\left(Y_{32}Y_{52}+Y_{33}Y_{53}\right)\left(2A^*_{21}+2A^*_{12}+A^*_{11}+3A^*_{22}\right),$$

$$G_{166}=\frac{Y_{31}}{a}\left(3C^*_{12}+C^*_{21}++B^*_{12}+3C^*_{22}+B^*_{11}+3B^*_{21}+3B^*_{22}+C^*_{11}\right)$$
$$-\frac{Y_{51}}{a^3}\left(B^*_{12}+C^*_{21}+B^*_{22}+C^*_{22}+3B^*_{11}+3C^*_{12}+3B^*_{21}+3C^*_{11}\right),$$

$$G_{167}=-Y_{31}\left(\Phi^*_{1r}+3\Phi^*_{1\theta}\right),G_{168}=2Y_{31}\left(2A^*_{21}+2A^*_{12}+3A^*_{22}+A^*_{11}\right),$$

$$G_{169}=2Y_{33}Y_{52}\left(2A^*_{21}+2A^*_{12}+3A^*_{22}+A^*_{11}\right)+\frac{16K_sH_{44}}{a^4},$$

$$G_{1610}=\frac{Y_{32}}{a}\left(3C^*_{12}+B^*_{12}+C^*_{21}+3C^*_{22}+B^*_{11}+3B^*_{21}+C^*_{11}+3B^*_{22}\right)$$
$$-\frac{Y_{53}}{a^3}\left(B^*_{12}+C^*_{21}+3C^*_{12}+C^*_{22}+3B^*_{11}+3B^*_{21}+B^*_{22}+3C^*_{11}\right),$$

$$G_{1611}=-Y_{32}\left(\Phi^*_{1r}+3\Phi^*_{1\theta}\right),G_{1612}=2Y_{32}\left(2A^*_{21}+2A^*_{12}+3A^*_{22}+A^*_{11}\right),G_{1613}=2Y_{33}\left(2A^*_{21}+2A^*_{12}+3A^*_{22}+A^*_{11}\right),$$

$$G_{1614} = -Y_{33}\left(\Phi_{1r}^{*} + 3\Phi_{1\theta}^{*}\right),$$

$$G_{1615} = \frac{Y_{33}}{a}\left(C_{11}^{*} + B_{12}^{*} + 3C_{12}^{*} + 3B_{22}^{*} + C_{21}^{*} + 3C_{22}^{*} + B_{11}^{*} + 3B_{21}^{*}\right) + \frac{Y_{53}}{a^3}\left(-3C_{11}^{*} - B_{12}^{*} - 3C_{12}^{*} - C_{21}^{*} - B_{22}^{*} - C_{22}^{*} - 3B_{11}^{*} - 3B_{21}^{*}\right) - \frac{8K_sH_{44}}{a^3},$$

$$G_{1616} = \frac{1}{a^3}\left(3\Phi_{2r}^{*} + \Phi_{2\theta}^{*}\right), G_{1617} = \frac{1}{a^3}\left(-3C_{12}^{*} - 3B_{11}^{*} - 3C_{11}^{*} - 3B_{21}^{*} - B_{22}^{*} - C_{21}^{*} - B_{12}^{*} - C_{22}^{*}\right),$$

$$G_{1618} = \frac{-6D_{11}^{*} - 4D_{12}^{*} - 4D_{21}^{*} - 2D_{22}^{*}}{a^4} + \frac{K_sH_{44}}{a^2},\quad G_{171} = Y_{51}^2\left(A_{21}^{*} + A_{12}^{*} + A_{22}^{*} + A_{11}^{*}\right),$$

$$G_{172} = 2Y_{51}Y_{53}\left(A_{21}^{*} + A_{12}^{*} + A_{22}^{*} + A_{11}^{*}\right),\quad G_{173} = 2Y_{51}Y_{52}\left(A_{21}^{*} + A_{12}^{*} + A_{22}^{*} + A_{11}^{*}\right),$$

$$G_{174} = Y_{53}^2\left(A_{21}^{*} + A_{12}^{*} + A_{22}^{*} + A_{11}^{*}\right),\qquad G_{175} = 2Y_{52}Y_{53}\left(A_{21}^{*} + A_{12}^{*} + A_{22}^{*} + A_{11}^{*}\right),$$

$$G_{176} = \frac{Y_{51}}{a}\left(B_{11}^{*} + B_{12}^{*} + C_{22}^{*} + B_{21}^{*} + B_{22}^{*} + C_{11}^{*} + C_{12}^{*} + C_{21}^{*}\right),\quad G_{177} = -Y_{51}\left(\Phi_{1r}^{*} + \Phi_{1\theta}^{*}\right),$$

$$G_{178} = 2Y_{51}\left(A_{21}^{*} + A_{12}^{*} + A_{22}^{*} + A_{11}^{*}\right),\qquad G_{179} = Y_{52}^2\left(A_{21}^{*} + A_{12}^{*} + A_{22}^{*} + A_{11}^{*}\right),$$

$$G_{1710} = \frac{Y_{53}}{a}\left(B_{11}^{*} + C_{22}^{*} + B_{12}^{*} + C_{21}^{*} + B_{22}^{*} + C_{11}^{*} + B_{21}^{*} + C_{12}^{*}\right),\ G_{1711} = -Y_{53}\left(\Phi_{1r}^{*} + \Phi_{1\theta}^{*}\right),$$

$$G_{1712} = 2Y_{53}\left(A_{21}^{*} + A_{12}^{*} + A_{22}^{*} + A_{11}^{*}\right),\qquad G_{1713} = 2Y_{52}\left(A_{21}^{*} + A_{12}^{*} + A_{22}^{*} + A_{11}^{*}\right),$$

$$G_{1714} = -Y_{52}\left(\Phi_{1r}^{*} + \Phi_{1\theta}^{*}\right),\quad G_{1715} = \frac{Y_{52}}{a}\left(C_{22}^{*} + B_{11}^{*} + C_{12}^{*} + B_{22}^{*} + C_{11}^{*} + B_{21}^{*} + C_{21}^{*} + B_{12}^{*}\right),$$

$$G_{1716} = -\frac{1}{a}\left(\Phi_{2r}^{*} + \Phi_{2\theta}^{*}\right),\quad G_{1717} = -\Phi_{1r}^{*} - \Phi_{1\theta}^{*},\quad G_{1718} = \frac{D_{12}^{*} + D_{22}^{*} + D_{11}^{*} + D_{12}^{*}}{a^2},$$

$$G_{1719} = \frac{1}{a}\left(C_{22}^{*} + B_{11}^{*} + B_{21}^{*} + C_{11}^{*} + B_{12}^{*} + C_{12}^{*} + B_{22}^{*} + C_{21}^{*}\right),\ G_{1720} = A_{12}^{*} + A_{21}^{*} + A_{22}^{*} + A_{11}^{*},$$

$$T_1 = \frac{1}{14}G_{111}a^{14} + \frac{1}{12}G_{121}a^{12} + \frac{1}{10}G_{131}a^{10} + \frac{1}{8}G_{141}a^{8} + \frac{1}{6}G_{151}a^{6} + \frac{1}{4}G_{161}a^{4} + \frac{1}{2}G_{171}a^{2},$$

$$T_2 = \frac{1}{14}G_{112}a^{14} + \frac{1}{12}G_{122}a^{12} + \frac{1}{10}G_{132}a^{10} + \frac{1}{8}G_{142}a^{8} + \frac{1}{6}G_{152}a^{6} + \frac{1}{4}G_{162}a^{4} + \frac{1}{2}G_{172}a^{2},$$

$$T_3 = \frac{1}{12}G_{123}a^{12} + \frac{1}{10}G_{133}a^{10} + \frac{1}{8}G_{143}a^{8} + \frac{1}{6}G_{153}a^{6} + \frac{1}{4}G_{163}a^{4} + \frac{1}{2}G_{173}a^{2},$$

$$T_4 = \frac{1}{14}G_{113}a^{14} + \frac{1}{12}G_{124}a^{12} + \frac{1}{10}G_{134}a^{10} + \frac{1}{8}G_{144}a^{8} + \frac{1}{6}G_{154}a^{6} + \frac{1}{4}G_{164}a^{4} + \frac{1}{2}G_{174}a^{2},$$

$$T_5 = \frac{1}{12}G_{125}a^{12} + \frac{1}{10}G_{135}a^{10} + \frac{1}{8}G_{145}a^{8} + \frac{1}{6}G_{155}a^{6} + \frac{1}{4}G_{165}a^{4} + \frac{1}{2}G_{175}a^{2},$$

$$T_6 = \frac{1}{10}G_{136}a^{10} + \frac{1}{8}G_{146}a^{8} + \frac{1}{6}G_{156}a^{6} + \frac{1}{4}G_{166}a^{4} + \frac{1}{2}G_{176}a^{2},$$

$$T_7 = \frac{1}{8}G_{148}a^{8} + \frac{1}{6}G_{158}a^{6} + \frac{1}{4}G_{168}a^{4} + \frac{1}{2}G_{178}a^{2},$$

$$T_8 = \left(\frac{1}{8}G_{147} - \frac{1}{8}Y_{11}A_{11}^*\Phi_{1r} - \frac{7}{8}Y_{11}A_{12}^*\Phi_{1r} - \frac{1}{8}Y_{11}A_{21}^*\Phi_{1\theta} - \frac{7}{8}Y_{11}A_{22}^*\Phi_{1\theta}\right)a^8$$
$$+\left(\frac{1}{6}G_{157} - \frac{1}{6}Y_{21}A_{11}^*\Phi_{1r} - \frac{5}{6}Y_{21}A_{12}^*\Phi_{1r} - \frac{1}{6}Y_{21}A_{21}^*\Phi_{1\theta} - \frac{5}{6}Y_{21}A_{22}^*\Phi_{1\theta}\right)a^6$$
$$+\left(\frac{1}{4}G_{167} - \frac{1}{4}Y_{31}A_{11}^*\Phi_{1r} - \frac{3}{4}Y_{31}A_{12}^*\Phi_{1r} - \frac{1}{4}Y_{31}A_{21}^*\Phi_{1\theta} - \frac{3}{4}Y_{31}A_{22}^*\Phi_{1\theta}\right)a^4$$
$$+\left(-\frac{1}{2}Y_{51}A_{22}^*\Phi_{1\theta} + \frac{1}{2}G_{177} - \frac{1}{2}Y_{51}A_{21}^*\Phi_{1\theta} - \frac{1}{2}Y_{51}A_{11}^*\Phi_{1r} - \frac{1}{2}Y_{51}A_{12}^*\Phi_{1r}\, a^2,\right.$$

$$T_9 = \frac{1}{10}G_{137}a^{10} + \frac{1}{8}G_{149}a^8 + \frac{1}{6}G_{159}a^6 + \frac{1}{4}G_{169}a^4 + \frac{1}{2}G_{179}a^2,$$

$$T_{10} = \frac{1}{10}G_{138}a^{10} + \frac{1}{8}G_{1410}a^8 + \frac{1}{6}G_{1510}a^6 + \frac{1}{4}G_{1610}a^4 + \frac{1}{2}G_{1710}a^2,$$

$$T_{11} = \frac{1}{8}G_{1412}a^8 + \frac{1}{6}G_{1512}a^6 + \frac{1}{4}G_{1612}a^4 + \frac{1}{2}G_{1712}a^2,$$

$$T_{12} = \left(\frac{1}{8}G_{1411} - \frac{1}{8}Y_{12}A_{11}^*\Phi_{1r} - \frac{7}{8}Y_{12}A_{12}^*\Phi_{1r} - \frac{1}{8}Y_{12}A_{21}^*\Phi_{1\theta} - \frac{7}{8}Y_{12}A_{22}^*\Phi_{1\theta}\right)a^8$$
$$+\left(-\frac{1}{6}\Phi_{1\theta}Y_{22}A_{21}^* - \frac{5}{6}Y_{22}A_{22}^*\overline{\Phi}_{1\theta} + \frac{1}{6}G_{1511} - \frac{1}{6}A_{11}^*\Phi_{1r}Y_{22} - \frac{5}{6}\Phi_{1r}Y_{22}A_{12}^*\, a^6\right.$$
$$+\left(\frac{1}{4}G_{1611} - \frac{1}{4}Y_{32}A_{11}^*\Phi_{1r} - \frac{3}{4}Y_{32}A_{12}^*\Phi_{1r} - \frac{1}{4}Y_{32}A_{21}^*\Phi_{1\theta} - \frac{3}{4}Y_{32}A_{22}^*\Phi_{1\theta}\right)a^4$$
$$+\left(-\frac{1}{2}Y_{53}A_{22}^*\Phi_{1\theta} + \frac{1}{2}G_{1711} - \frac{1}{2}Y_{53}A_{21}^*\Phi_{1\theta} - \frac{1}{2}Y_{53}A_{11}^*\Phi_{1r} - \frac{1}{2}A_{12}^*Y_{53}\Phi_{1r}\, a^2,\right.$$

$$T_{13} = \frac{1}{8}G_{1413}a^8 + \frac{1}{6}G_{1515}a^6 + \frac{1}{4}G_{1615}a^4 + \frac{1}{2}G_{1715}a^2,\quad T_{14} = \frac{1}{6}G_{1513}a^6 + \frac{1}{4}G_{1613}a^4 + \frac{1}{2}G_{1713}a^2,$$

$$T_{15} = \left(-\frac{5}{6}A_{12}^*Y_{23}\Phi_{1r} + \frac{1}{6}G_{1514} - \frac{5}{6}Y_{23}\Phi_{1\theta}A_{22}^* - \frac{1}{6}Y_{23}\Phi_{1r}A_{11}^* - \frac{1}{6}Y_{23}\Phi_{1\theta}A_{21}^*\right)a^6$$
$$+\left(\frac{1}{4}G_{1614} - \frac{1}{4}Y_{33}A_{11}^*\Phi_{1r} - \frac{1}{4}A_{21}^*Y_{33}\Phi_{1\theta} - \frac{3}{4}Y_{33}\Phi_{1\theta}A_{22}^* - \frac{3}{4}Y_{33}\Phi_{1r}A_{12}^*\right)a^4$$
$$+\left(\frac{1}{2}G_{1714} - \frac{1}{2}Y_{52}\Phi_{1r}A_{11}^* - \frac{1}{2}Y_{52}\Phi_{1r}A_{12}^* - \frac{1}{2}Y_{52}\Phi_{1\theta}A_{21}^* - \frac{1}{2}Y_{52}\Phi_{1\theta}A_{22}^*\right)a^2,$$

$$T_{16} = \frac{1}{8}G_{1414}a^8 + \frac{1}{6}G_{1516}a^6 + \frac{1}{4}G_{1618}a^4 + \frac{1}{2}G_{1718}a^2,\qquad T_{17} = \frac{1}{4}G_{1617}a^4 + \frac{1}{2}G_{1719}a^2,$$

$$T_{18} = \frac{G_{1616}a^4}{4} + \frac{G_{1716}a^2}{2} + \left(\frac{1}{4}\pi\Phi_{1\theta}B_{21}^* + \frac{1}{4}\pi\Phi_{1r}B_{11}^* - \frac{1}{4}\pi\Phi_{1r}B_{12}^* + \frac{1}{4}\pi\Phi_{2r} - \frac{1}{4}\pi\Phi_{2\theta} - \frac{1}{4}\Phi_{1\theta}\pi B_{22}^*\right)a,$$

$$T_{19} = \frac{G_{1720}a^2}{2},\quad T_{20} = \left(-\frac{1}{2}\Phi_{1\theta}A_{21}^*\frac{1}{2}G_{1717} - \frac{1}{2}A_{12}^*\Phi_{1r} - \frac{1}{2}A\Phi_{1\theta}A_{22}^* - \frac{1}{2}\Phi_{1r}A_{11}^*\right)a^2,$$

$$T_{21} = \frac{a^2}{2}\left(\Phi_{1r}\Phi_{1r}^* + \Phi_{1\theta}\Phi_{1\theta}^*\right),\ N_1 = -\frac{2\pi a^2}{9},\ N_2 = -\frac{a^2}{5},\ N_3 = -\frac{4}{3},\ N_4 = \frac{a^2}{3},$$